Staging of Non-small Cell Lung Cancer

8

Gregor Sommer and Mark N. Wiese

Abstract

The process of lung cancer staging is getting increasingly complex and requires distinct input from specialized physicians of radiology, nuclear medicine, thoracic surgery, and pathology. Also after the advent of the revised 8th edition of the TNM classification, noninvasive imaging with CT and ^{18}F-FDG-PET, supplemented by MRI, continues to provide the initial basis for clinical staging by determining the anatomic extent of the disease and thus plays a pivotal role in the diagnosis and management of NSCLC. In cases without distant metastatic disease, pretherapeutic mediastinal staging with invasive methods (mediastinoscopy or endoscopic procedures) is mandatory to determine the most appropriate treatment strategy if imaging findings are positive or in certain scenarios that come along with a high risk of false-negative imaging results. The most important limitation inherent to the current TNM staging system is its purely anatomic character that provides insufficient information related to the many different sorts of novel targeted therapies. This translates also to imaging-derived staging of NSCLC in radiology and nuclear medicine, where—besides higher anatomic resolution and image quality—the most important remaining challenge is to gather more "functional" information and generate a more comprehensive picture of the disease by noninvasive staging methods.

Keywords

Non-small cell lung cancer · Neoplasm staging
TNM classification · Positron-emission tomography · Computed tomography
Magnetic resonance imaging · Mediastinoscopy
Endoscopic ultrasonography

8.1 Development and Evaluation of T, N, and M Descriptors

Lung cancer is the most common cancer worldwide accounting for nearly 13% of all newly diagnosed cancers in 2012 [1]. With almost 20% of all cancer-related deaths it is also the most common cause of death from cancer despite substantial improvements in diagnosis, therapy, and prevention in the last decades. Non-small cell lung cancer (NSCLC) is by far the most often occurring type of lung cancer with a proportion of 83.4% [2].

G. Sommer (✉)
Clinic of Radiology and Nuclear Medicine, University Hospital Basel, University of Basel, Basel, Switzerland
e-mail: gregor.sommer@usb.ch

M. N. Wiese
Clinic of Thoracic Surgery, University Hospital Basel, University of Basel, Basel, Switzerland
e-mail: mark.wiese@usb.ch

M. Anzidei, M. Anile (eds.), *Diagnostic Imaging for Thoracic Surgery*,
https://doi.org/10.1007/978-3-319-89893-3_8

Staging of cancer describes the diagnostic process of gathering all pieces of information relevant to define the extent of the disease of an individual patient. Correct staging is crucial both for defining the prognosis of the patient and for selecting the most appropriate therapy. Imaging has developed as an important contributor to this assessment at initial diagnosis, as well as during post-interventional follow-up. As for most solid tumors, staging of NSCLC follows the TNM (tumor, node, metastasis) formula, which has initially been proposed by Denoix in 1946 [3] and has been accepted shortly after by the Union Internationale Contre le Cancer (UICC) and the American Joint Committee on Cancer (AJCC) as the official system for coding the anatomic extent of the disease.

Although staging is most commonly performed in the context of the initial diagnosis, it can also take place at other significant points of time in the history of a cancer patient. Thus, along with the TNM formula, it's important to record in which context the tumor stage has been defined. For this purpose, prefixes are applied to distinguish between the clinical stage (cTNM), the pathological stage (pTNM), post-therapeutic stages (yc/ypTNM), tumor stages at the time of progression or recurrence (rTNM), and the stage at autopsy (aTNM).

Table 8.1 summarizes the TNM descriptors for lung cancer as applied in the 8th edition of the TNM system [5] that came into effect on January 1st 2017. As the 7th edition [6], the 8th edition of the TNM classification applies to all histopathological subtypes of NSCLC, to small-cell carcinoma and to atypical carcinoids.

The T descriptor denotes the extent of the primary tumor by describing its morphological features like size and location, rates the involvement of adjacent anatomic structures, and reports the presence of separate tumor nodules in the lung. As compared to the T descriptors in the 7th edition, the T categories in the 8th edition were further refined by introducing two new size cut points at 1 and 4 cm. This refinement was made also with respect to the increasing numbers of screening detected cancers. Also, a new category for minimally invasive adenocarcinoma (T1(mi)) was added. Moreover, tumors between 5 and 7 cm in size were

Table 8.1 T, N, and M descriptors for the 8th edition of TNM classification for lung cancer

Descriptor	Definition	
T: Primary tumor		
T*x*		Primary tumor cannot be assessed or tumor proven by presence of malignant cells in sputum or bronchial washings but not visualized by imaging or bronchoscopy
T0		No evidence of primary tumor
Tis		Carcinoma in situ
T1		Tumor ≤3 cm in greatest dimension, surrounded by lung or visceral pleura, without invasion more proximal than the lobar bronchus
	T1(mi)	**Minimally invasive adenocarcinoma**[a]
	T1a	**Tumor ≤1 cm in greatest dimension**[b]
	T1b	**Tumor >1 cm but ≤2 cm in greatest dimension**[b]
	T1c	**Tumor >2 cm but ≤3 cm in greatest dimension**[b]
T2		Tumor >3 cm **but ≤5 cm** or with any of the following features[c]: – **Involves main bronchus regardless of distance from the carina but without involvement of the carina** – Invades visceral pleura – **Associated with atelectasis or obstructive pneumonitis that extends to the hilar region, involving part or all of the lung**
	T2a	**Tumor >3 cm but ≤4 cm in greatest dimension**
	T2b	**Tumor >4 cm but ≤5 cm in greatest dimension**
T3		**Tumor >5 cm but ≤7 cm in greatest dimension** or associated separate tumor nodule(s) in the same lobe as the primary tumor or directly invades any of the following structures: chest wall (including the parietal pleura and superior sulcus tumors), phrenic nerve, parietal pericardium
T4		Tumor >7 cm in greatest dimension or associated with separate tumor nodule(s) in a different ipsilateral lobe than that of the primary tumor or invades any of the following structures: **diaphragm**, mediastinum, heart, great vessels, trachea, recurrent laryngeal nerve, esophagus, vertebral body, and carina

Table 8.1 (continued)

Descriptor	Definition	
N: Regional lymph node involvement		
N*x*		Regional lymph nodes cannot be assessed
N0		No regional lymph node metastasis
N1		Metastasis in ipsilateral peribronchial and/or ipsilateral hilar lymph nodes and intrapulmonary nodes, including involvement by direct extension
N2		Metastasis in ipsilateral mediastinal and/or subcarinal lymph node(s)
N3		Metastasis in contralateral mediastinal, contralateral hilar, ipsilateral or contralateral scalene, or supraclavicular lymph node(s)
M: Distant metastasis		
M0		No distant metastasis
M1		Distant metastasis present
	M1a	Separate tumor nodule(s) in a contralateral lobe; tumor with pleural or pericardial nodule(s) or malignant pleural or pericardial effusion[d]
	M1b	**Single extrathoracic metastasis[e]**
	M1c	**Multiple extrathoracic metastases in one or more organs**

Changes to the 7th edition are in bold
Reprinted from [4] with permission from Elsevier
[a]Solitary adenocarcinoma, ≤3 cm with a predominately lepidic pattern and ≤5 mm invasion in any one focus
[b]The uncommon superficial spreading tumor of any size with its invasive component limited to the bronchial wall, which may extend proximal to the main bronchus, is also classified as T1a
[c]T2 tumors with these features are classified as T2a if ≤4 cm in greatest dimension or if size cannot be determined, and T2b if >4 cm but ≤5 cm in greatest dimension
[d]Most pleural (pericardial) effusions with lung cancer are due to tumor. In a few patients, however, multiple microscopic examinations of pleural (pericardial) fluid are negative for tumor and the fluid is nonbloody and not an exudate. When these elements and clinical judgment dictate that the effusion is not related to the tumor, the effusion should be excluded as a staging descriptor
[e]This includes involvement of a single distant (nonregional) lymph node

adjusted in terms of prognosis (now classified as T3 instead of T2b), and some reassignments were made concerning tumor invasion to the diaphragm (now classified as T4) and the main bronchus within 2 cm of the carina (now classified as T2).

The N descriptor reports about the absence, presence, and location of locoregional lymph node metastases, which strongly affects the extensiveness of therapy and the prognosis of the patient. For this reason, N staging may be regarded as the most important component of intrathoracic staging. N staging is based on a standardized lymph node map (Fig. 8.1) that assigns any thoracic lymph node to a defined anatomic zone. The different stations and zones can be separated following clear anatomic landmarks assessable on cross-sectional imaging (see also Sect. 8.2.1). This lymph node map has been officially released by the International Association for the Study of Lung Cancer (IASCL) along with the 7th edition of the TNM classification [7] and is a combination and further development of the two previously used maps proposed by Mountain and Dresler [8] and the Japan Lung Cancer Society [9]. Using this map, N stage is defined by the most remote metastatic lymph node with respect to the location of the primary tumor. N descriptors of the 8th edition are unchanged compared to the 7th edition. However, a subclassification based on the number of involved nodes in N1 and N2 stations has been proposed for testing to enable potential refinements in future revisions (not contained in Table 8.1).

The M category finally describes the absence, presence, and location of distant metastases. Here, the 8th edition introduced a new M category to distinguish the rare but prognostically favorable cases with one single extrathoracic metastasis (new M1b) from those with multiple extrathoracic metastases (new M1c). The category M1a, as before, describes intrathoracic metastases in the contralateral lung, pleura, or pericardium.

As for other tumors, optional descriptors of prognostic relevance as listed in Table 8.2 may be used along with the TNM descriptors in the classification. These include the grade of differentiation (G); the absence or presence of perineural, lymphatic, or vascular invasion (Pn, L, and V); and the completeness of surgical tumor resection (R).

It is important to be aware that the T, N, and M classifiers describe the extent of disease only in respect to anatomic criteria. The key role of a

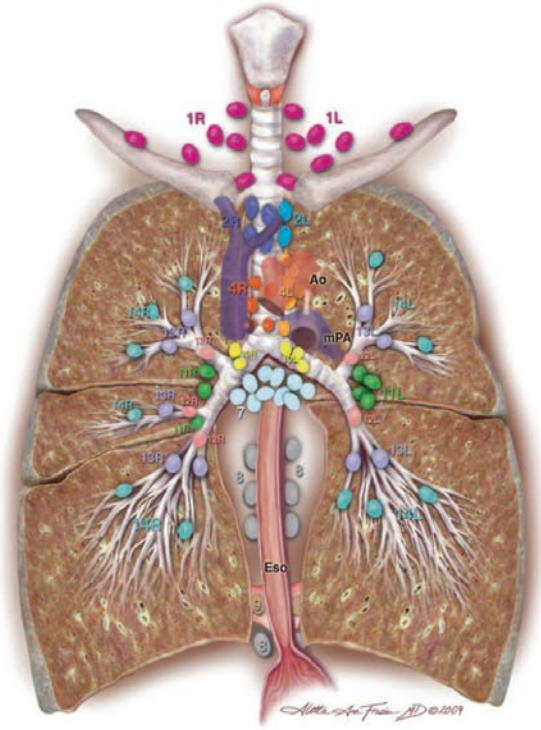

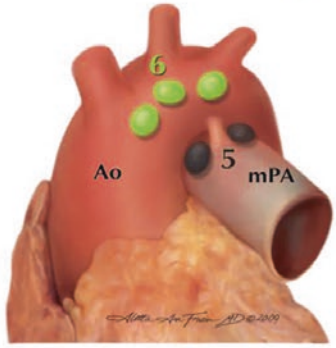

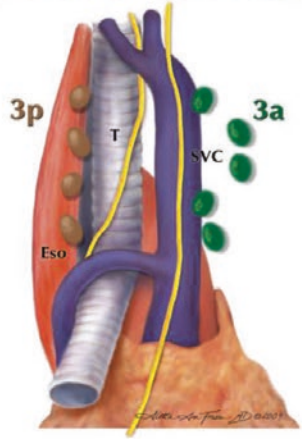

Supraclavicular zone
- 1 Low cervical, supraclavicular, and sternal notch nodes

SUPERIOR MEDIASTINAL NODES

Upper zone
- 2R Upper Paratracheal (right)
- 2L Upper Paratracheal (left)
- 3a Prevascular
- 3p Retrotracheal
- 4R Lower Paratracheal (right)
- 4L Lower Paratracheal (left)

AORTIC NODES

AP zone
- 5 Subaortic
- 6 Para-aortic (ascending aorta or phrenic)

INFERIOR MEDIASTINAL NODES

Subcarinal zone
- 7 Subcarinal

Lower zone
- 8 Paraesophageal (below carina)
- 9 Pulmonary ligament

N1 NODES

Hilar/Interlobar zone
- 10 Hilar
- 11 Interlobar

Peripheral zone
- 12 Lobar
- 13 Segmental
- 14 Subsegmental

Fig. 8.1 The International Association for the Study of Lung Cancer (IASLC) lymph node map, including the proposed grouping of lymph node stations into "zones" for the purposes of prognostic analyses. Reprinted from [7] with permission from Elsevier

classification system for cancer, however, is to translate this anatomic information into prognostic information. For this purpose, so-called prognostic groups are derived from the anatomic TNM descriptors. These prognostic groups are also referred to as the UICC tumor stages and form the core element of the TNM classification system. It is obvious that TNM descriptors and stage groupings need to be continuously adapted to the ever-changing conditions in lung cancer diagnosis and therapy. The stage groupings of the 8th edition of the TNM classification are shown in Table 8.3. Changes from the 7th edition include the introduction of several new subcategories for stage IA (subdivided into IA1–3), stage III (new category IIIC), and stage IV (subdivided into IVA and IVB). In addition, some of the TNM groups have been relocated into a different stage, which are T1 N1 M0 (former IIA, now IIB), T2a N1 M0 (former IIA, now IIB), and T3 N2 M0 (former IIIA, now IIIB). An overview on the effect of the refined stage grouping in terms of overall survival is given in Fig. 8.2.

Table 8.2 Optional descriptors of prognostic relevance to be used with the TNM classification [5]

Optional TNM descriptors		
G		Grade of differentiation
	G1	Well differentiated
	G2	Moderately differentiated
	G3	Poorly differentiated
	G4	Undifferentiated
Pn		Perineural invasion
	Pn0	No perineural invasion
	Pn1	Perineural invasion
L		Lymphatic invasion
	L0	No lymphatic invasion
	L1	Lymphatic invasion
V		Vascular invasion
	V0	No venous invasion
	V1	Microscopic venous invasion
	V2	Macroscopic venous invasion
R		Completeness of resection
	R0	No residual tumor
	R1	Microscopic residual tumor
	R2	Macroscopic residual tumor

The UICC published its first edition of the TNM Classification of Malignant Tumors in 1958. It has been revised seven times until the proposals for the 8th edition of the TNM classification were published in 2015 and 2016 [4, 10, 11]. By consensus between the UICC and the AJCC, efforts were made from the beginning to avoid publication of different classifications. Editions 2–6 of the UICC manual on the TNM Classification of Malignant Tumors were based on a continuously growing database of patients

Table 8.3 Definition of UICC stages from the TNM descriptors according to the 8th edition of the TNM staging system for NSCLC [4]

UICC stage	TNM Descriptors			
Occult carcinoma	T*x* N0 M0			
0	Tis N0 M0			
IA1	T1(mi) N0 M0 T1a N0 M0			
IA2	T1b N0 M0			
IA3	T1c N0 M0			
IB	T2a N0 M0			
IIA	T2b N0 M0			
IIB	T3 N0 M0	T1a-c N1 M0 T2a-b N1 M0		
IIIA	T4 N0 M0	T3 N1 M0 T4 N1 M0	T1a-c N2 M0 T2a-b N2 M0	
IIIB			T3 N2 M0 T4 N2 M0	T1a-c N3 M0 T2a-b N3 M0
IIIC				T3 N3 M0 T4 N3 M0
IVA	M1a-b (any T, any N)			
IVB	M1c (any T, any N)			

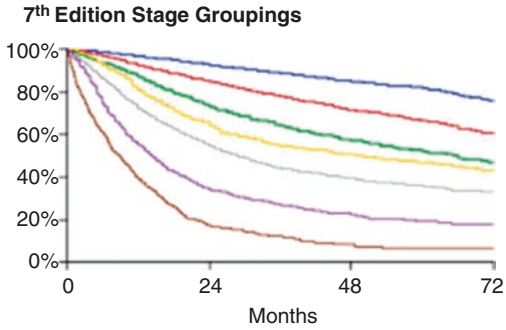

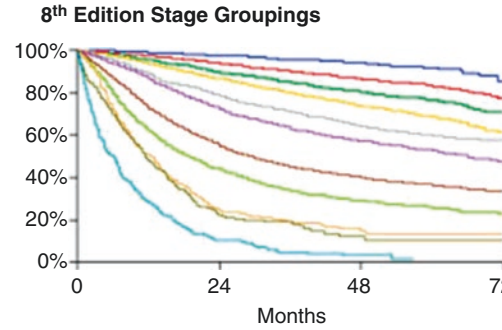

7th Ed.	Events / N	MST	24 Month	60 Month
IA	1119 / 6303	NR	93%	82%
IB	768 / 2492	NR	85%	66%
IIA	424 / 1008	66.0	74%	52%
IIB	382 / 824	49.0	64%	47%
IIIA	2139 / 3344	29.0	55%	36%
IIIB	2101 / 2624	14.1	34%	19%
IV	664 / 882	8.8	17%	6%

Proposed 8th Ed.	Events / N	MST	24 Month	60 Month
IA1	68 / 781	NR	97%	92%
IA2	505 / 3105	NR	94%	83%
IA3	546 / 2417	NR	90%	77%
IB	560 / 1928	NR	87%	68%
IIA	215 / 585	NR	79%	60%
IIB	605 / 1453	66.0	72%	53%
IIIA	2052 / 3200	29.3	55%	36%
IIIB	1551 / 2140	19.0	44%	26%
IIIC	831 / 986	12.6	24%	13%
IVA	336 / 484	11.5	23%	10%
IVB	328 / 398	6.0	10%	0%

Fig. 8.2 Overall survival by clinical stage according to the 7th edition and the proposed 8th edition groupings using the entire database available for the 8th edition. MST, median survival time. Survival is weighted by type of database submission: registry versus other. Reprinted from [4], with permission from Elsevier

Table 8.4 Comparison of the databases used for the 6th, 7th, and 8th editions of the TNM classification for lung cancer [13, 14]

	TNM 6	TNM 7	TNM 8
Evaluation period	1975–1988	1990–2000	1999–2010
Number of patients	5319	100,869	94,708
Number of institutions/databases	Mainly single center	45	35
Origin	US only	58% Europe 21% North America 12% Asia 9% Australia	49% Europe 5% North America 44% Asia 2% Australia

that was essentially collected and managed by Dr. Clifton Mountain at the University of Texas, MD Anderson Cancer Center, with contributions from the United States National Cancer Institute Cooperative Lung Cancer Study Group. By the time of the editions 5 and 6 (which were of identical content) in 1997 and 2002, this database included 5319 patients, 4351 of them originating from MD Anderson. Despite its considerable size, the fact of using a patient database stemming predominantly from a single institution to create an "international" staging classification was subject to increasing criticism at that time. In consequence, the 7th edition of the TNM classification for lung cancer enacted in January 2010 was the first to be developed under the roof of the IASCL, which was founded in 1974 as the only global organization dedicated to the study of lung cancer. To overcome the limitations of the 6th edition, the IASCL lung cancer staging project

[12] with its subcommittees for T, N, and M components, stage grouping, validation, SCLC, carcinoids, visceral pleura invasion, lymph node map, and nonanatomic prognostic factors established and evaluated an international database to include patients treated in different healthcare systems and a broad spectrum of therapeutic modalities (Table 8.4). This broad international concept was followed also for the 8th edition. Its new database included 94,708 cases of lung cancer diagnosed between 1999 and 2010 at 35 institutions in 16 countries, treated with all sorts of therapeutic procedures [15].

8.2 Radiologic Diagnosis

8.2.1 Computed Tomography (CT)

Computed tomography is the most commonly applied imaging examination in patients with suspected lung cancer. It is used either in the first instance in cases of various suspected pulmonary pathologies or as the second-line modality following an abnormal chest X-ray. It also has an emerging role as a screening test for individuals at high risk.

CT scans for staging purposes, i.e., examinations of patients with proven or at least strongly suspected lung cancer, should be performed after intravenous injection of an iodine-based contrast agent. The scan range should cover the entire chest from the supraclavicular areas to the upper abdomen to allow for the assessment of the liver and adrenal glands. A section thickness of less than 1.5 mm with contiguous or overlapping slices is recommended [16]. Images should be reconstructed using soft-tissue and lung reconstruction kernels. Multiplanar reconstruction is essential to determine the size of tumor (Fig. 8.3), differentiate between nodules and scars, and describe the extent of the tumor with respect to anatomical landmarks, e.g., its distance to the pleural surface or to the carina. Additional thin-section maximum intensity projection (MIP) reconstruction is considered helpful for the detection of smaller pulmonary nodules.

8.2.1.1 Tumor Detection

The primary task of CT in lung cancer management is to detect any lesion suspicious for lung cancer and describe its exact location. In this context, CT serves as an essential guide to biopsy, either by CT-guided needle biopsy, bronchoscopy, or surgery. The reported performance of low-dose CT applied for detection of lung cancer in the framework of two large lung cancer screening trials is summarized in Table 8.5.

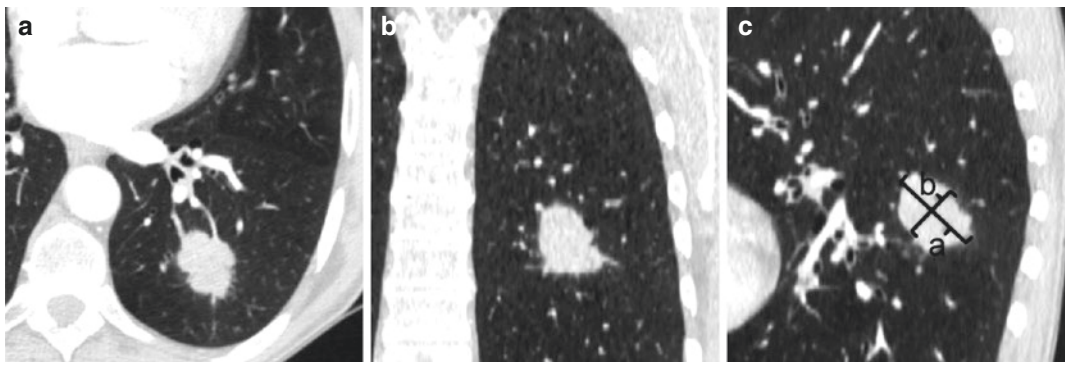

Fig. 8.3 CT of a pulmonary adenocarcinoma in the left lower lobe superior segment. Reformats in three dimensions (**a**: axial, **b**: coronal, **c**: sagittal) are necessary to determine the size of the tumor and describe its exact location for biopsy. Note that size measurements for the management of incidentally detected pulmonary nodules and tumor staging are different: While the first is determined by the average of long- and short-axis diameters on the image that reveals the greatest dimensions ((*a* + *b*)/2 rounded to the nearest whole millimeter) [16], the latter is determined by the longest diameter of the tumor in three dimensions (**b**). For part-solid nodules, the maximum diameters of both the solid component (→T stage) and the entire lesion should be reported [17]

Table 8.5 Performance of low-dose CT for detection of lung cancer in the framework of lung cancer screening

	NLST		NELSON	
	Value (%)	95% CI (%)	Value (%)	95% CI (%)
Sensitivity	93.8	90.6–96.3	84.6	79.6–89.2
Specificity	73.4	72.8–73.9	98.6	98.5–98.8
PPV	52.9[a]	48.4–57.4[a]	40.4	35.9–44.7
NPV	99.9	99.86–99.94	99.8	99.8–99.9

NLST National Lung Screening Trial [18]; *NELSON* NEderlands Leuvens Longkanker Screenings ONderzoek [19]; *PPV* Positive predictive value; *NPV* Negative predictive value
[a]PPV for any positive finding that led to a biopsy procedure

8.2.1.2 T Staging

CT has the highest spatial resolution among all imaging modalities for measuring tumor size. It is therefore the method of choice to analyze the extent of the disease using the size cutoffs of the TNM classification as a reference. This applies particularly to the assessment of the earlier T stages (T1a–T2b). For staging purposes, the longest dimension of the tumor in the three axes must be reported (Fig. 8.3). For part-solid lesions, T stage is determined based on the solid component of the lesion [17], but the size of the non-solid component should be reported as well. Volumetric assessment may increase the measurement accuracy in the context of screening, assessment of incidentally found unspecified pulmonary nodules, and therapy monitoring. Staging of locally advanced lung cancer (T3 and T4) may be challenging with CT alone, as it can describe some, but not all, of the features that characterize these stages. Consequently, the reliability of CT for predicting T3/T4 disease is relatively poor [20]. Typical features that are evident on CT are, for instance, the presence of satellite nodules, crossing of the tumor through fissures (Fig. 8.4), tumor infiltration to the main bronchus or the carina (Fig. 8.5), and an involvement of bones, evident as lytic or sclerotic changes (Fig. 8.6). The presence of atelectasis, pneumonia, and carcinomatous lymphangitis may be seen as well. An exact differentiation between such changes and the tumor, however, can be difficult even on contrast-enhanced scans, and FDG uptake in PET may serve as a helpful guide in this context. Regarding invasion of vascular structures or organs, the integrity of the fatty layers around the vessel or organ is a strong indicator in terms of resectability. On the other hand, the absence of such layers must not be taken as a proof of vascular infiltration, unless the entire circumference of the vessel is enclosed by the tumor (Fig. 8.7) or there is evidence of endovascular tumor growth. Another difficult diagnosis is invasion of the pleura outside the fissures. Here, only a visible penetration *through* the pleural surface with signs of infiltration of adjacent structures (e.g., ribs, mediastinal fat) may be counted as infiltration, while simple contact of the tumor with the pleura or pleural effusion does not prove pleural invasion. In cases of doubt, particularly concerning a suspected infiltration of the chest wall and mediastinum on CT, MRI is a potential modality to provide more clarity (see below). The reported accuracy of CT for T staging is 68% overall [21] and varies from 43% in T3 tumors to 81% in T1 and T2 tumors and 88% in T4 tumors [22].

8.2.1.3 N Staging

Lymph node involvement in NSCLC is assessed and documented based on the IASCL lymph node map displayed above (Fig. 8.1). Notably, N stage is only determined by the anatomic extent, i.e., by the fact whether or not an anatomic zone is affected, but not by the number or size of the affected lymph nodes in each station. Dedicated manuals are available on how to make the assignment of a suspicious node to one of the 14 lymph node stations and 7 anatomic zones using anatomic landmarks on CT [23]. An important such landmark is, for instance, the left lateral wall of the trachea that—instead of the anatomic midline—separates the right from the left mediastinal zones. While CT is very exact in assigning individual lymph nodes to a particular station or zone, its accuracy to differentiate benign from malignant lymph nodes is limited: The

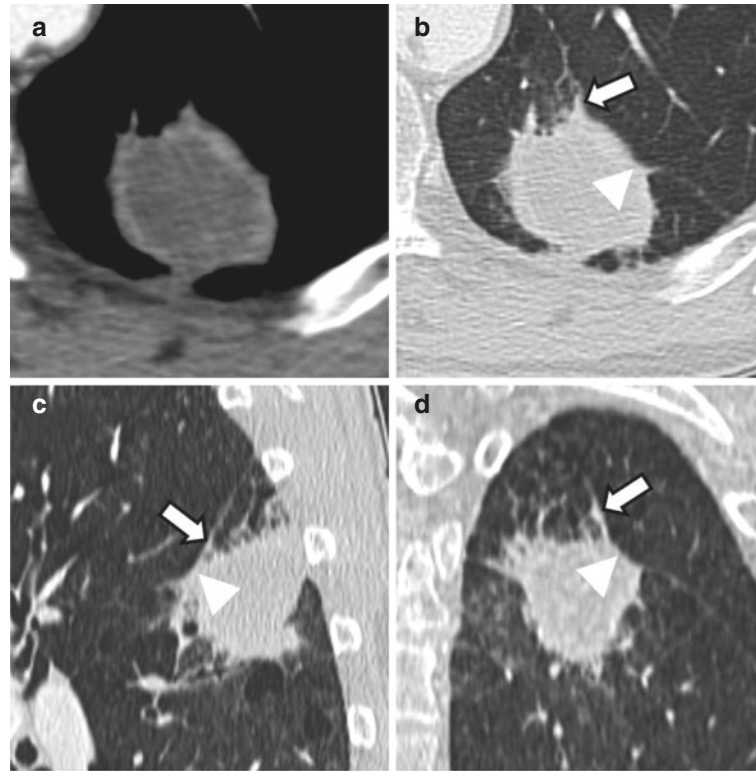

Fig. 8.4 Adeno carcinoma of the left lower lobe superior segment with evident invasion of the visceral pleura on CT. (**a**) Soft-tissue window, transverse section; (**b**–**d**) lung window in transverse (**b**), sagittal (**c**), and coronal view (**d**). The tumor has a maximum diameter of 44 mm and shows retraction (*arrowheads*) and thickening (*arrows*) of the adjacent fissure as signs of visceral pleura invasion. The combination of both features finally classifies the tumor as stage T2b

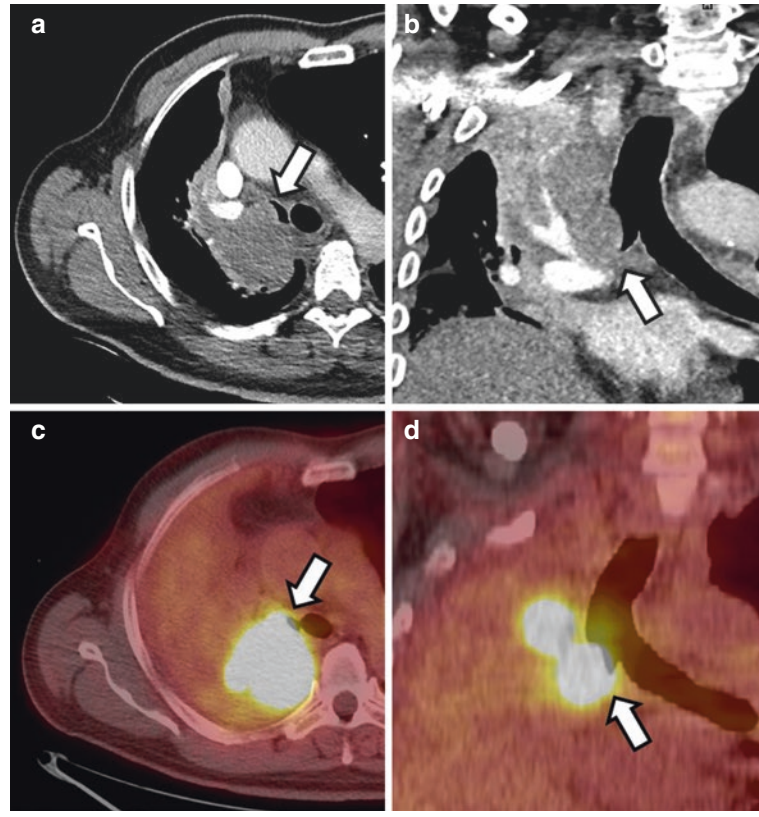

Fig. 8.5 Infiltration of the main bronchus in a 58-year-old man with pulmonary squamous cell carcinoma stage cT3 cN2 cM1b. (**a**, **b**) Contrast-enhanced CT; (**c**, **d**) FDG-PET/CT with non-enhanced CT acquired 2 days after the initial CT exam. A hypermetabolic mass (*arrows*) is noted invading the right main bronchus with a remaining distance of less than 2 cm to the carina. Note that the distance threshold of 2 cm separating the stages T2 and T3 in the 7th edition is not included anymore in the 8th edition of the TNM classification

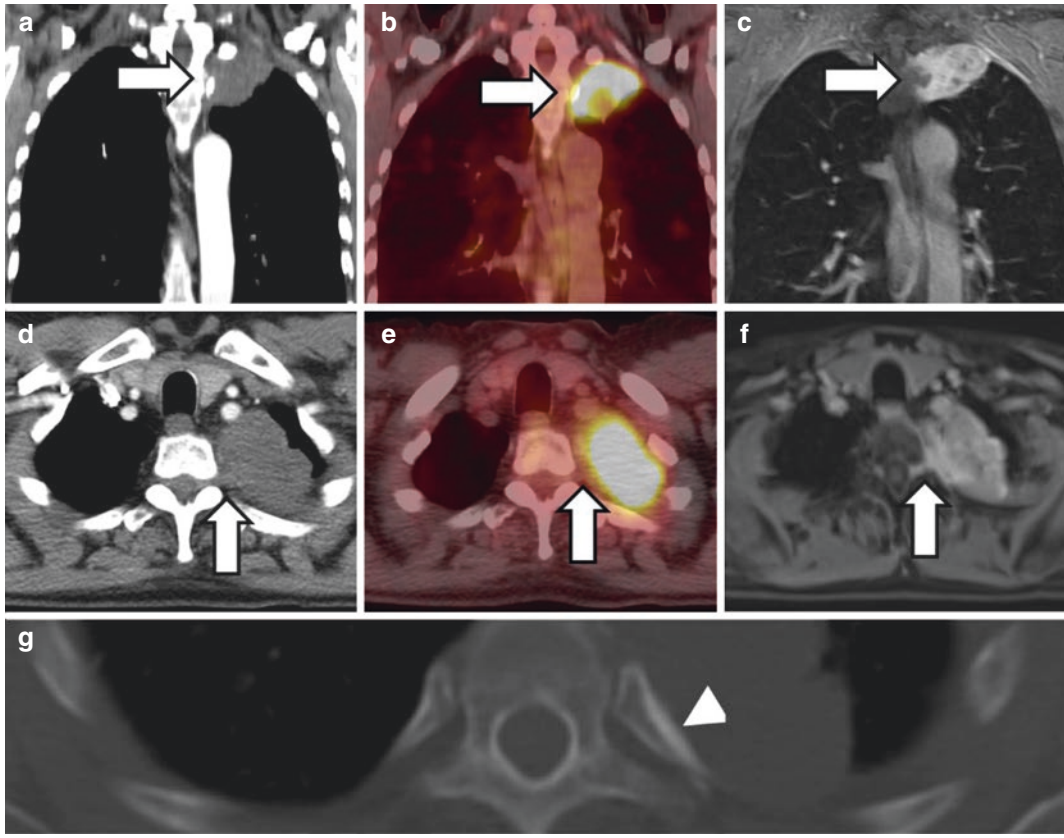

Fig. 8.6 NSCLC of the left upper lobe apicoposterior segment with infiltration of the paravertebral space and adjacent neuroforamina Th2 and Th3. Evidently, the process of tumor invasion (*arrows*) is much better visualized with MRI (fat-suppressed T1-weighted gradient echo post-contrast, **c** and **f**) as compared to contrast-enhanced CT (**a**, **d**) and FDG-PET/CT (**b**, **e**). Note, however, the presence of a sclerotic periosteal reaction at the head of the third rib on the left side as a sign of tumor invasion in CT (*arrowhead* in **g**)

reported sensitivity and specificity for detecting mediastinal lymph node metastases with CT alone do not exceed 51% and 81%, respectively [24]. This limitation mainly originates from the fact that the key CT feature for malignancy is size: Usually, a short-axis diameter of 10 mm is taken as the cut-off value to differentiate benign from malignant lymph nodes [24]. It is well known, however, that microscopic lymph node metastases may be present also in lymph nodes of normal size, while on the other hand lymph node enlargement may be caused by inflammation, as well. Thus, the use of size cutoffs on CT leads to approximately 40% false-positive diagnoses (benign nodes >1 cm) and 20% false-negative diagnoses (malignant lymph nodes <1 cm) [25–27].

8.2.1.4 M Staging

M staging is a very important issue also in NSCLC, as the presence of distant metastases strongly limits the available treatment options and thus significantly lowers the prognosis of the patient. About 40% of the NSCLC patients do have a distant metastasis at the time of initial diagnosis [28]. In approximately 90% of these patients, the disease manifests itself through specific symptoms of metastatic spread, particularly in cases of bone or brain metastases. CT as the number one imaging modality in emergency radiology plays a pivotal role in these cases. The situation is different in cases without clinical evidence of metastatic disease at the time of initial diagnosis. Here, the focus is on the exclusion of

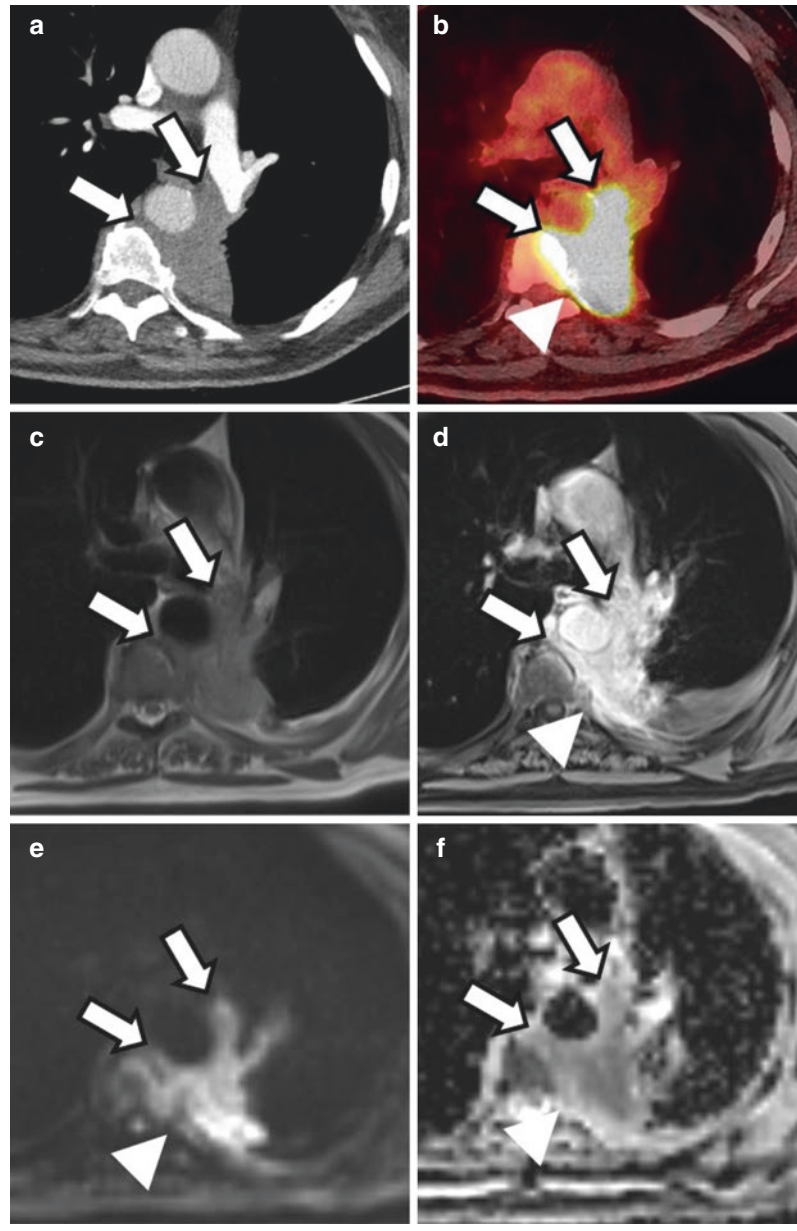

Fig. 8.7 Assessment of mediastinal invasion from NSCLC with CT (**a**), FDG-PET/CT (**b**), and MRI (**c**–**f**), including T2-weighted fast spin-echo (**c**), contrast-enhanced fat-suppressed T1-weighted gradient echo (**d**), diffusion-weighted MRI with *b*-value = 800 s/mm^2 (**e**), and ADC map (**f**). A centrally located, strongly hypermetabolic tumor is seen in the left lower lobe extending towards the mediastinum, surrounding half of the circumference of the thoracic aorta (*arrows*). In addition, osseous infiltration of the adjacent rib and vertebral body is noted in PET and MRI (*arrowhead*)

metastases in order to assign the patient to a curative treatment strategy. As for primary tumor detection, the sensitivity and negative predictive value of CT to detect or rule out tumor nodules in the contralateral lung (M1a metastatic disease) are unsurpassed by other modalities. The diagnostic value of CT for the detection of pleural metastases can be limited by the presence of pleural effusion. The sensitivity and specificity of CT for the detection of metastases to the bone, liver, and adrenals are reasonable, but inferior to combined FDG-PET/CT (see below). The pooled sensitivity and specificity for the detection of brain metastases with contrast-enhanced CT are reported as 73% (95% CI, 60–83%) and 85% (95% CI, 72–92%), respectively [24]. This is less compared with MRI, but accepted as a method to exclude brain metastases if MRI is not available.

8.2.2 ^{18}F-Fluorodeoxyglucose-Positron-Emission Tomography/Computed Tomography (FDG-PET/CT)

Positron-emission tomography (PET) is a nuclear imaging modality used to detect and localize radioactive β^+ decay. In comparison to scintigraphy and single-photon-emission computed tomography (SPECT), PET has a higher spatial resolution (≈5 mm) and detection efficiency. PET works with numerous tracers that are marked with β^+ emitters. By far the most important one is ^{18}F-2-fluor-2-deoxy-D-glucose (^{18}F-FDG), which is an analogue of D-glucose and, as such, mimics the glucose uptake into the cells. Like D-glucose, FDG is taken up into the cells via the glucose transporter molecules (GLUT) and becomes phosphorylated inside the cell by the enzyme hexokinase. The phosphorylated FDG, unlike D-glucose, cannot be processed further and thus accumulates inside the cell, while it decays with a half-life time of 110 min. The known pharmacokinetics allow expressing the FDG uptake in each voxel as quantitative numbers using the standardized uptake value (SUV), thereby enabling a quantitative assessment of the metabolic activity of tissues and particularly malignant tumors. A general SUV cutoff that characterizes malignancy does not exist, as the intensity of FDG uptake depends on several factors such as tumor histology, volume of vital tumor cells, movement of the target lesion during the acquisition, and physiological uptake of the adjacent background [29]. Having been developed and applied historically as separate techniques, PET and CT have been integrated more than a decade ago into one modality, named PET/CT. The particular strength of PET/CT is the synergetic effect of a functional imaging method (PET) that offers a high sensitivity for the detection of malignant tissue and a morphology-based imaging method (CT) highly accurate in describing the anatomic location and extent of affected structures. In consequence, FDG-PET/CT is the most powerful noninvasive examination tool for staging of NSCLC available today [30]. PET is not developed or sold as a stand-alone technology anymore, and only rarely used as such. Nevertheless, much data on the accuracy of FDG-PET for staging of NSCLC is still considered valid and provides parts of the basis of the current guidelines.

Patient preparation and data acquisition for FDG-PET follow standardized examination protocols as published in the procedure guidelines of the European Association for Nuclear Medicine (EANM) [29]. The imaging agent ^{18}F-FDG is administered intravenously in a predefined dose that is adapted to the patient's body weight. Patients must respect a fasting period of at least 6 h before administration. Eventually, images are acquired after a resting period of 60 min after the injection of the radiopharmaceutical. For lung cancer, an extended torso scan ranging from the top of the skull to the mid-thigh is recommended. The patient's arms must be elevated during the procedure. Along with the PET, a CT scan of the chest and upper abdomen should be performed as described in 8.2.1 if no recent chest CT exam of sufficient quality is available. Otherwise a non-contrast-enhanced low-dose CT protocol for attenuation correction and anatomic reference is considered sufficient.

8.2.2.1 Tumor Detection

The role of FDG-PET/CT in the context of tumor detection is that of a tool for stratification of pulmonary nodules with intermediate probability of malignancy. As such, FDG-PET/CT has been shown to decrease the number of futile invasive biopsies and thoracotomies [31]. Due to the high sensitivity of FDG-PET, a negative FDG-PET result can rule out malignancy reliably in the majority of pulmonary lesions. Exceptions to this rule are nodules smaller than 10 mm and non-solid solitary pulmonary nodules, which should be followed up by CT in a structured program [16]. A final diagnosis of cancer is not possible based on a positive FDG-PET result alone due to the limited specificity of the exam (82% according to [32]). An invasive histopathological or cytological proof of malignancy is therefore mandatory in any PET-positive finding. False-positive findings in FDG-PET are known to occur

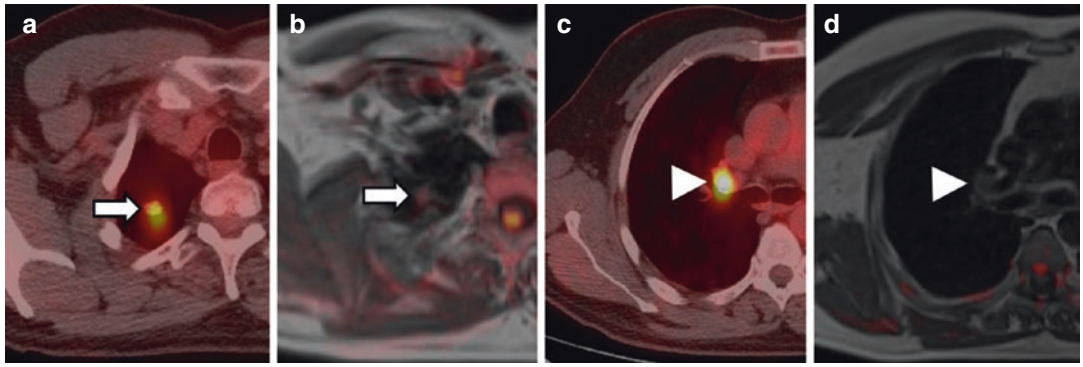

Fig. 8.8 False-positive findings in FDG-PET/CT in a patient with primary tuberculosis. (**a**, **c**) FDG-PET/CT; (**b**, **d**) hybrid images from diffusion-weighted MRI ($b = 800$ s/mm^2) and T1-weighted fast spin-echo MRI. The PET/CT was rated false positive for malignancy (T1a N1, UICC IIA (TNM 7)) due to high FDG uptake in both the primary lesion (**a**) and in a right hilar lymph node (**c**). On the MRI exam (performed in the same patient within the framework of a prospective trial) only slightly restricted diffusion is noted within the primary lesion (**b**) and no suspicious lymphadenopathy is seen (**d**). Figure adapted from [33], with permission

particularly in the presence of infectious, inflammatory, or granulomatous diseases (Fig. 8.8).

8.2.2.2 T Staging

FDG-PET/CT is a better overall predictor for T stage than FDG-PET or CT alone. The reported staging accuracy across all T stages is 82% for PET/CT versus 55% for PET alone and 68% for CT alone (pooled average over eight studies published between 2003 and 2007 [20]). As for CT, the staging accuracy of FDG-PET/CT depends on the tumor stage and is worst for T3 (45%), followed by stages T1/T2 (81%) and T4 (83%) [22]. Regarding the prognostically most relevant identification of T3 and T4 disease, varying sensitivities and specificities can be found in literature. These range from 38% to 90% and from 40% to 90%, respectively, for the detection of parietal pleural or chest wall invasion, and from 40% to 84% and from 57% to 94%, respectively, for mediastinal tumor invasion [21]. While PET can reliably differentiate tumor from atelectasis (which is commonly FDG negative), it has limited capability to differentiate tumor from pneumonia and carcinomatous lymphangitis. Other assets of hybrid FDG-PET/CT for T staging are to detect or rule out secondary tumor nodules in the ipsilateral lung (stages T3 and T4) and identify tumor invasion into vessels, organs, or bones by increased metabolism (Figs. 8.6 and 8.7).

8.2.2.3 N Staging

N staging is the particular strength of FDG-PET, as the mechanism of highlighting the tumor tissue by its increased glucose metabolism allows identifying cancer infiltration also in normal sized lymph nodes (Fig. 8.9). This leads to a significantly higher sensitivity of FDG-PET (77%) compared to CT (55%) with also slightly higher specificity of 86% (CT 81%) [24]. An even higher increase in sensitivity and specificity results from the combination of both modalities with numbers of 80–90% sensitivity and 85–95% specificity for hybrid FDG-PET/CT [20]. FDG-PET/CT, in particular, allows ruling out metastatic spread to locoregional lymph nodes with a very high negative predictive value of 88–95% [27] and thus helps avoiding invasive staging procedures. Limitations of FDG-PET/CT for N staging are known, however, for three particular scenarios [20]: The first is in patients with suspected N1 disease (central tumor or positive N1 lymph node in PET/CT and otherwise normal mediastinum). In these patients, who have an intermediate suspicion of N2 and N3 involvement, the false-negative rate of FDG-PET/CT for N2 and N3 disease is around 30%. The second scenario refers to cases

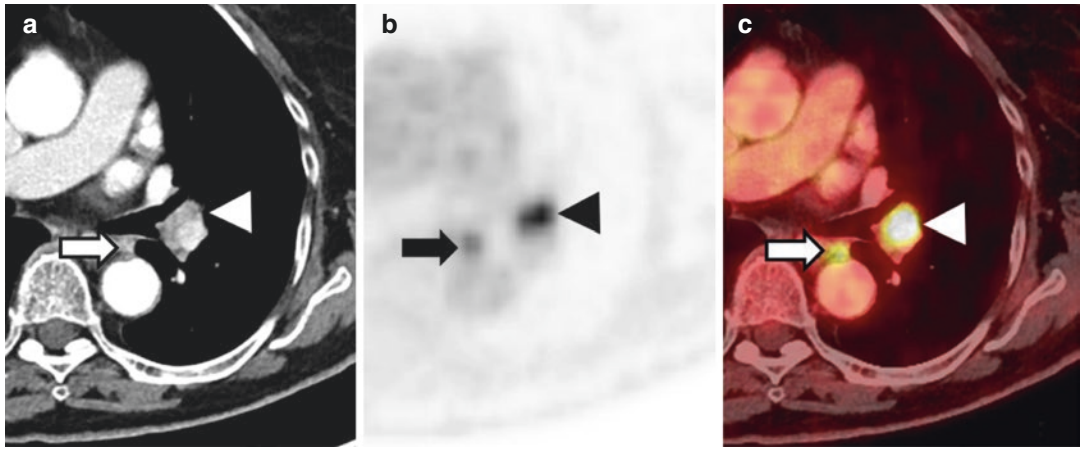

Fig. 8.9 High sensitivity of FDG-PET demonstrated in a case of adenocarcinoma originating from the left lower lobe with N2 disease involving lymph nodes at the left hilum (visibly enlarged at CT, *arrowhead*) and a normal sized node in the left mediastinum hardly visible on CT (*arrow*). (**a**) contrast-enhanced CT, (**b**) FDG-PET, (**c**) hybrid FDG-PET/CT

where the size of the primary tumor is larger than >3 cm and the NPV for mediastinal lymph node involvement goes down to 85–89%. The third scenario is that of a central tumor with negative appearance in FDG-PET. Here, the reported false-negative rate for assessment of lymph node involvement with FDG-PET/CT is as high as 21.6%. All patients who are affected by one of the three scenarios mentioned are recommended to undergo invasive staging of the mediastinum. In any case, patients who have a positive finding on FDG-PET/CT that is suspicious for a lymph node metastasis need to have this finding confirmed by tissue sampling. This is due to the considerable number of false positives occurring in FDG-PET from infection or inflammation that limit the positive predictive value of FDG-PET and PET/CT to 75% and 63%, respectively [24].

8.2.2.4 M Staging

The most common locations for extrathoracic metastatic spread are the brain, bone, liver, and adrenal glands. FDG-PET/CT is considered the superior imaging technology for detecting these metastases on a whole-body level and it has been shown that PET scanning discloses previously unsuspected metastases in 6–37% of cases [24]. As for the T and N stages, the particular strength of FDG-PET/CT is its high negative predictive value that allows ruling out metastatic disease with high accuracy, thereby reducing the number of futile treatment trials [31]. An exception from this rule applies particularly to scans of the brain, where the sensitivity of FDG-PET is limited by the high background FDG uptake of the brain and consequently MRI or contrast-enhanced CT is preferred (Fig. 8.10). Regarding the detection of bone metastases, FDG-PET is reported to have an excellent performance with specificity, sensitivity, NPV, PPV, and accuracy all above 90%, surpassing also radionuclide bone scanning [34, 35]. Adrenal masses are a relatively common finding occurring in approximately 5% of patients without known malignancy [36] and the vast majority of these lesions are known to be benign adenomas. The prevalence of adrenal metastases from NSCLC increases with the intrathoracic extent of the tumor [37]. Accuracy values as high as 100% have been reported for FDG-PET to detect these adrenal metastases. False negatives, however, may occur in small lesions, and false positives have also rarely been described. MRI, especially with chemical shift and contrast-enhanced techniques, may be useful in case of uncertainty (Figs. 8.11 and 8.12). The prevalence of benign liver lesions, mainly cysts and hemangiomas, in the general population is even higher than that of adrenal masses and reaches 15% in large-scale

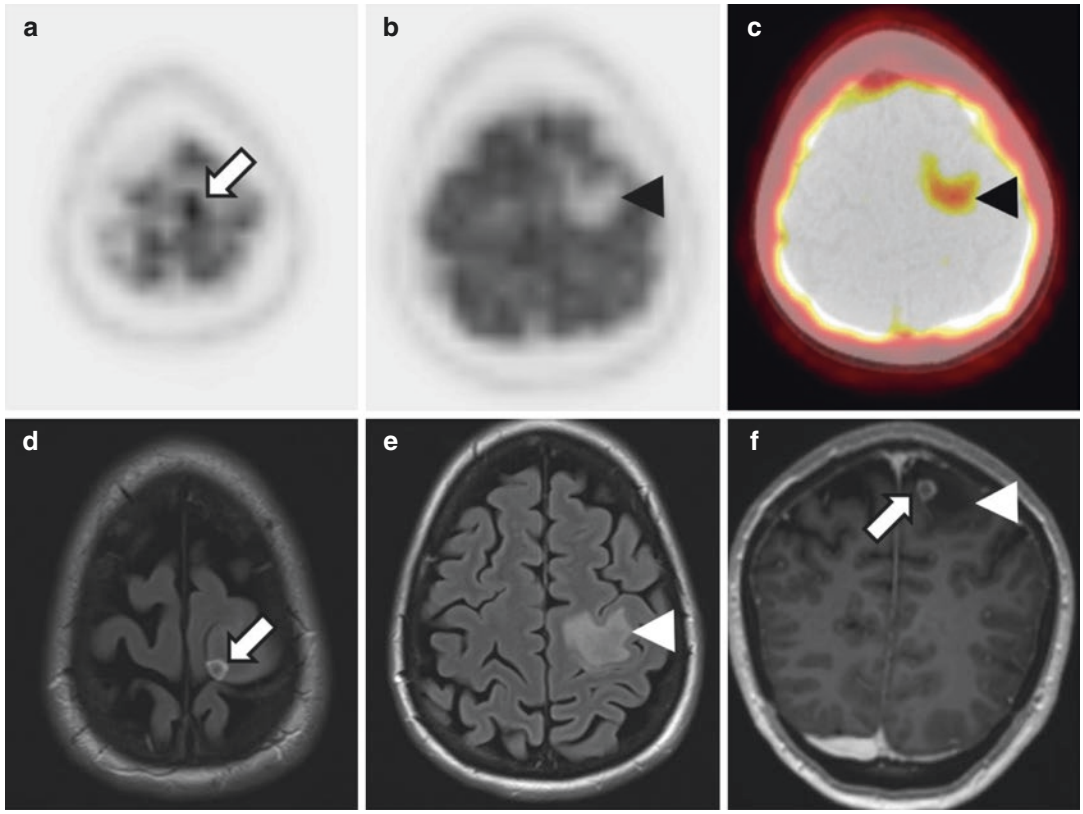

Fig. 8.10 Brain metastasis detected in a 43-year-old woman with NSCLC (not otherwise specified) stage UICC IV. (**a**, **b**) FDG-PET; (**c**) hybrid PET/CT image; (**d**, **e**) T2-weighted fluid-attenuated inversion recovery (FLAIR), (**f**) T1w gradient-echo post-Gd. The presence of this small brain metastasis in the cortex of the left precentral gyrus (*arrows*) becomes mainly evident through the effect of its surrounding edema (*arrowheads*). The lesion itself is hardly visible on FDG-PET (**a**), due to the physiologic FDG uptake of the surrounding cortex. In contrast, MRI (**d**, **f**) provides a much better differentiation of the lesion against the background both using T2-weighted and contrast-enhanced techniques

ultrasound studies [38]. In contrast, the frequency of liver metastases in asymptomatic patients with NSCLC is reported to be only 3% [39]. FDG-PET can detect liver metastases from NSCLC with a very high accuracy of 92–100% and only few false positives [40]. The further characterization of any unclear FDG-negative liver lesions remains the domain of ultrasound, contrast-enhanced CT, and MRI.

According to the guidelines of the American College of Chest Physicians (ACCP) and the European Society of Thoracic Surgery (ESTS), FDG-PET is recommended as the imaging modality of choice to evaluate for metastases in patients with a normal clinical evaluation and no suspicious extrathoracic abnormalities on chest CT being considered for treatment with curative intent. It is not indicated for patients already classified as non-curative by CT or other imaging. In patients with an imaging finding suggestive of a metastasis, further evaluation of the abnormality with tissue sampling is recommended to pathologically confirm the clinical stage prior to choosing treatment [24].

8.2.3 Magnetic Resonance Imaging

Magnetic resonance imaging (MRI) is a method for cross-sectional imaging that is available in clinical routine since the 1980s. Methodically, it is based on the fact that the magnetic properties of protons,

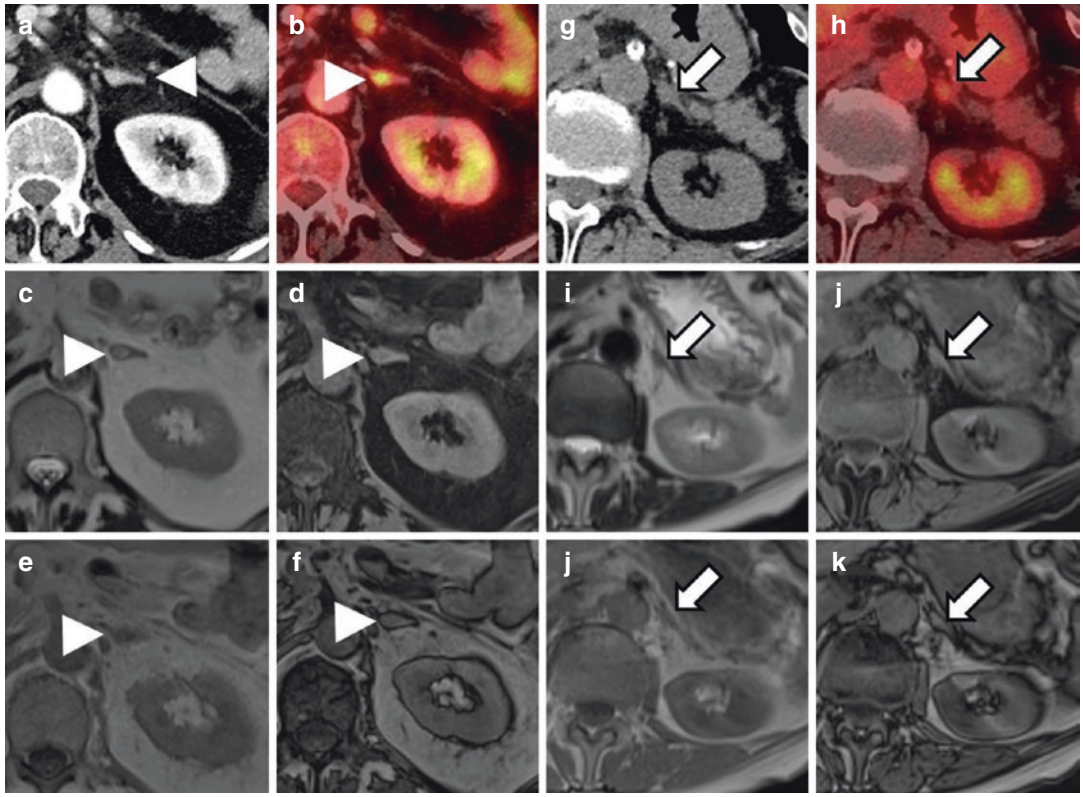

Fig. 8.11 True- and false-positive findings of small adrenal lesions in FDG-PET/CT and MRI. (**a**–**f**) Adrenal metastasis in a patient with pulmonary adenocarcinoma stage T1b N1. The lesion is too small to be noticed on contrast-enhanced CT (**b**), but identified by its increased uptake of FDG (SUV_{max} = 5.0) in PET (**a**). MRI confirms the finding showing a hyperintense lesion in T2-weighted fast spin echo (**c**) with slightly less contrast enhancement compared to the surrounding adrenal tissue in fat-suppressed T1-weighted gradient-echo post-contrast (**d**) and no signal drop in opposed-phase (**e**) compared to in-phase gradient echo (**f**). (**g**–**l**) Nodular thickening of the left adrenal of another patient with stage T2a N2 pulmonary adenocarcinoma in CT (**g**) showing faint uptake (SUV_{max} = 3.1) of FDG in PET (**h**). MRI, however, showed an entirely normal signal behavior of the left adrenal (**i**–**l**, sequences as described in **c**–**f**), ruling out adrenal metastasis in this patient

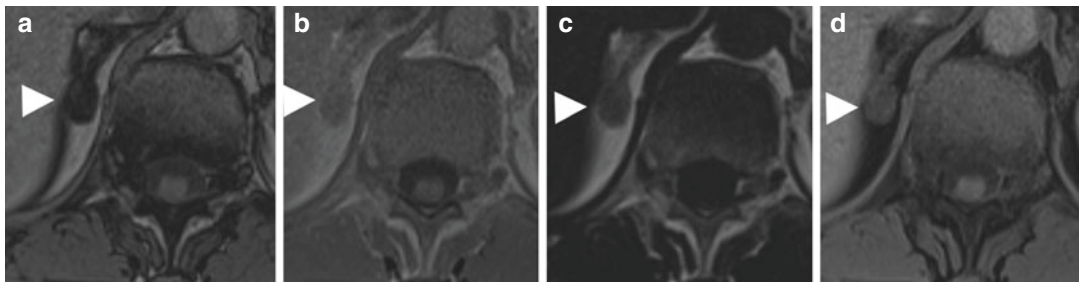

Fig. 8.12 Typical signal characteristics of an adrenal adenoma (*arrowheads*) in T1-weighted Dixon MRI at 1.5 T field strength: (**a**) Opposed-phase image (echo time = 2.4 ms); (**b**) in-phase image (echo time = 4.8 ms); (**c**) fat image (after Dixon reconstruction); (**d**) water image (after Dixon reconstruction). As adrenal adenomas contain fat in a microscopic distribution (i.e., the size of fat deposits is far below the voxel resolution of the MRI), this fat is not seen macroscopically (dark appearance of the adenoma in (**c**)), but can only be identified indirectly by chemical shift effects that cause a drop of >20% in signal intensity in the opposed-phase image (**a**) compared to the in-phase image (**b**)

which are bound to water or other molecules in human tissue, vary depending on their physical and biochemical environment. Static and variable magnetic fields are used to interact with this magnetization and display its spatial distribution in the body. The particular strength of MRI is its ability to generate different sorts of contrast for tissue characterization, such as T1 weighting, T2 weighting, diffusion-weighted MRI (DW-MRI), or contrast enhancement from intravenously administered, gadolinium-based contrast agents. The various MRI methods may be applied either alone (within a protocol including T1-weighted, T2-weighted, diffusion-weighted, and contrast-enhanced sequences), or in combination with FDG-PET within hybrid FDG-PET/MRI approaches. The first is widely available at least in larger hospitals and is described below. Hybrid PET/MR, which still has limited clinical availability, is further discussed in the Sect. 8.4 at the end of this chapter.

8.2.3.1 Tumor Detection

As the sensitivity of MRI for the detection of pulmonary nodules is considerably lower than that of CT, it is not an accepted method to rule out pulmonary malignancy in patients with clinically suspected cancer. Nevertheless, there is some discussion about a potential role of MRI as a tool for lung cancer screening where the repetitive radiation exposure associated with CT is an issue [41].

8.2.3.2 T Staging

The accuracy of MRI for T staging has already been investigated in studies from the early 1990s [42]. These reported a comparable sensitivity and specificity of MRI (56% and 80%) and CT (63% and 84%) in distinguishing T3–T4 tumors from T1–T2 tumors using standard MRI sequences such as T2 and T1 weighting. MRI was found, in particular, to be significantly more accurate than CT in the diagnosis of mediastinal invasion (Figs. 8.6 and 8.7), whereas no significant differences were found between the two techniques for diagnosis of bronchial involvement or chest wall invasion. These results have been corroborated also in a recent randomized study of 263 patients comparing post hoc co-registered whole-body FDG-PET/MRI and FDG-PET/CT [43]. According to the current guidelines [24], MRI should not be performed routinely for staging of the mediastinum, but is considered useful when there is concern about involvement of the superior sulcus or the brachial plexus.

8.2.3.3 N Staging

The additional benefit of morphologic MRI protocols over CT for nodal staging is generally limited, as both methods basically rely on size and shape as the main imaging criteria. Interesting additional options have been provided by two research groups from Japan [44, 45], who described their methods based on short TI inversion recovery (STIR) turbo spin-echo sequences to be superior to FDG-PET/CT for N staging of lung cancer (91.4% vs. 80.7% accuracy as reported by [44]). Another very promising MRI technique is diffusion-weighted MRI (DW-MRI), which has been adapted to whole-body oncologic imaging by Takahara in 2004 [46] and identifies cancer metastases by their dense microstructure that restricts the diffusion of water molecules (Fig. 8.13). The most recent meta-analysis on the diagnostic performance of FDG-PET/CT and DW-MRI for detection of mediastinal nodal metastasis in NSCLC based on 43 studies found no significant difference between the two modalities [47]. The pooled sensitivity and specificity for FDG-PET/CT were 65% (95% CI: 63–67%) and 93% (93–94%), respectively, whereas the corresponding values of DW-MRI were 72% (68–76%) and 97% (96–98%), respectively. Despite these positive results, a general recommendation for using STIR or DW-MRI routinely for staging of NSCLC has not yet been made, as data from large prospective studies comparing their value with that of FDG-PET are still missing [20].

8.2.3.4 M Staging

The most important role of MRI for M staging of NSCLC staging is the detection or exclusion of brain metastases (Fig. 8.11), where MRI represents the standard of reference for clinical staging. The overall prevalence of brain metastases in clinically asymptomatic patients with NSCLC is very low, with 3% on average [24], but increases to >20% in

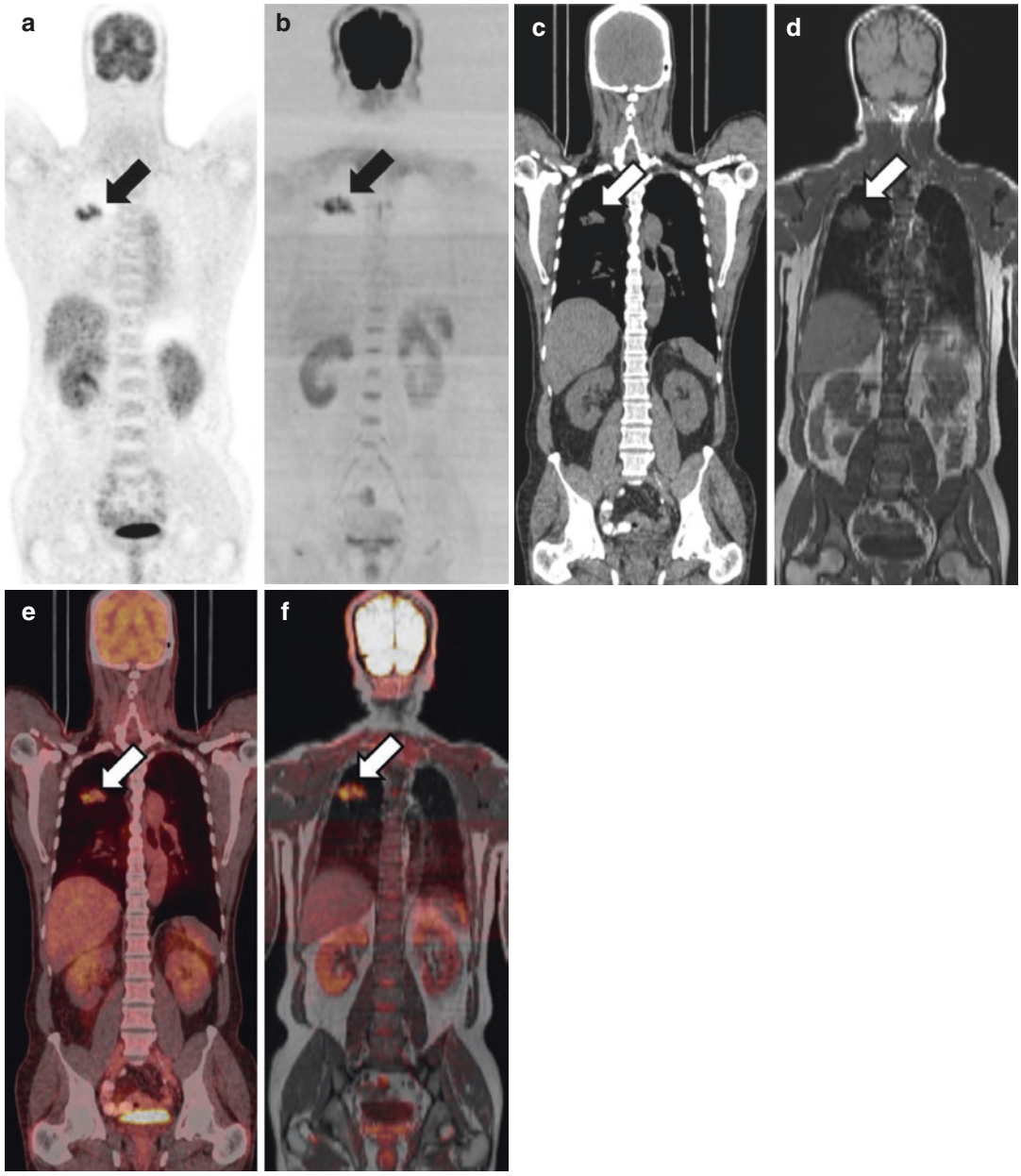

Fig. 8.13 Side-by-side comparison of FDG-PET/CT (right) and whole-body MRI (left) in a patient with pulmonary squamous cell carcinoma stage T2a N0 M0 showing comparable image contrast of the tumor in the right upper lobe with both methods. (**a**) FDG-PET; (**b**) diffusion-weighted MRI (b = 800 s/mm^2); (**c**) CT (soft-tissue window); (**d**) T1w fast spin-echo MRI; (**e**, **f**) hybrid images after fusion of **a/c**, and **b/d**, respectively. MRI data were acquired as 2D slices in transverse orientation

stage III and IV diseases [48] or with primary tumor size >3 cm [49]. As shown already in studies from the 1990s [50], MRI is able to detect more and smaller lesions than contrast-enhanced CT in the preoperative setting. However, it has not yet been proven that this technical advantage translates into a significant effect on patient survival. The current guidelines recommend performing routine imaging of the brain with MRI in clinically symptomatic patients and in patients with clinical stage III or IV NSCLC, even if they have a negative clinical evaluation [24]. The guidelines give no general recommendation to use MRI to detect or exclude metastases from NSCLC outside the brain, due to the good performance of FDG-PET/CT in these areas. In particular, there is no recommendation to use whole-body MRI techniques, such as DW-MRI (Fig. 8.13) for M staging, despite some promising results that have been presented recently (98.6% reported accuracy of assessment of distant metastatic spread with DW-MRI according to [44]). MRI is accepted, nevertheless, as a problem-solving tool to characterize unclear lesions in the liver and help with the differential diagnosis of suspicious adrenal lesions (Figs. 8.11 and 8.12).

8.2.4 Bone Scintigraphy

Bone scintigraphy, also known as bone scan, is a traditional method of nuclear medicine used to detect and display pathologic alterations of bone metabolism. It uses γ-emitting substances like ^{99m}Tc-methyl-diphosphonate (MDP) that are adsorbed to the surface of bone in places of increased bone matrix turnover after intravenous injection. Images are acquired 2–4 h after injection of the radiotracer as 2-dimensional anterior and posterior projection

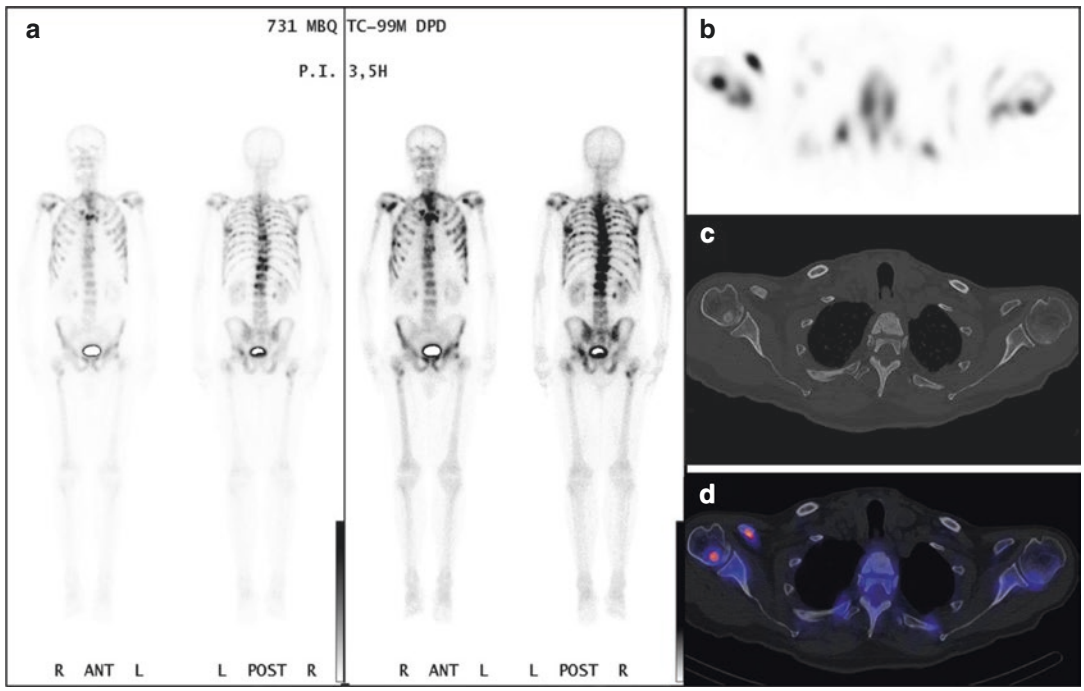

Fig. 8.14 Bone scan performed in a 72-year-old patient with pulmonary adenocarcinoma stage cT2a cN3 cM1b with evidence of bone metastases. (**a**) Planar scintigraphy in anterior and posterior projection with two different window/level settings; (**b**) SPECT, transverse image orientation; (**c**) CT, bone window; (**d**) hybrid SPECT/CT. Though the mechanism of tracer accumulation is per se unspecific, the pattern of distribution mostly allows identifying metastatic disease already on planar scintigraphy (**a**). Combined SPECT/CT (**b**–**d**) is used to differentiate metastatic from degenerative disease more specifically and to evaluate pathologic fractures

views (Fig. 8.14), supplemented by focal planar projection images or 3-dimensional SPECT acquisitions in particularly suspicious areas [51]. Bone scintigraphy has a relatively high diagnostic sensitivity for bone metastases from NSCLC of 92.5% [35], but is very sensitive to degenerative, traumatic, and inflammatory changes of the skeleton, as well. Due to this lack in specificity, bone scintigraphy only has a moderate accuracy of 72.5% for skeletal M staging that is significantly inferior to the 93.5% of FDG-PET [35]. In consequence, bone scintigraphy is not recommended anymore for evaluation of bone metastases in patients with NSCLC since the era of FDG-PET/CT. Nevertheless, it may still be used in combination with a thoracoabdominal CT in institutions where PET is not available.

8.3 Correlation with Surgical Staging

Pretherapeutic mediastinal staging has a central role in determining the most appropriate treatment strategy in cases of NSCLC without metastatic disease. Even if imaging findings are positive, microscopic confirmation of malignancy and histopathological type are required in all cases. In cases of doubt, the 8th edition of the Union for International Cancer Control (UICC) TNM staging system should be adopted to accurately determine tumor stage. The majority of cases of UICC stage IIA to IIIA NSCLC with N1 lymph node involvement are resectable. However, curative surgery is not possible for stage IIIB disease. In recent years, it has become clear that N2 staging is complex. Therefore, in such cases, differentiation should be improved by using the Robinson classification [52] in addition to TNM staging. Single-level stage IIIA-N2 NSCLC is suitable for surgery, either initially or after neoadjuvant therapy, while cases of multilevel N2-IIIA disease should preferentially undergo neoadjuvant therapy before surgery. However, bulky-N2 stage disease is considered inoperable. In the following, a short review of the currently available invasive procedures for mediastinal staging is provided. Table 8.6 provides an overview on their sensitivity, specificity, NPV, and PPV in comparison to CT, PET, and PET/CT. The current ESTS guidelines for primary mediastinal staging of NSCLC are referenced at the end of this subchapter.

8.3.1 Mediastinoscopy

Due to its high sensitivity and specificity, mediastinoscopy and especially video-assisted mediastinoscopy (VMS) are considered to be the gold standard technique for invasive mediastinal lymph node staging/diagnosis. Several factors can influence mediastinoscopy results. Not every lymph node localization that is important for staging can be reached by standard mediastinoscopy methods (Table 8.7). Lymph nodes in the aortopulmonary window (APW; station 5) and anterior mediastinal (station 6), posterior subcarinal (station 7), and inferior mediastinal (stations 8 and 9), hilar (station 10), and lobar/intralobar (stations 11–14) areas cannot be accessed by standard mediasti-

Table 8.6 Performance of different locoregional staging techniques (adapted from [53])

	Sensitivity (%)	Specificity (%)	NPV (%)	PPV (%)
CT	57	82	83	56
PET	84	89	93	79
Combined PET/CT [20, 27]	80–90	85–95	88–95	83–93
Mediastinoscopy (standard)	81	100	91	100
Mediastinoscopy (incl. ECM/VAMLA) [54]	96	100	100	100
Blind TBNA	76	96	71	100
EBUS-TBNA [55]	88	100	85	100
EUS-FNA	88	91	77	98
Combined EBUS-TBNA/EUS-FNA [54, 56]	86–88	99–100	83	99

NPV Negative predictive value; *PPV* Positive predictive value; *TBNA* Transbronchial needle aspiration; *EBUS* Endobronchial ultrasound; *EUS* Endoscopic ultrasound; *FNA* Fine-needle aspiration

Table 8.7 Accessibility of mediastinal lymph node stations to different invasive procedures

Procedure	Accessible lymph node stations
Mediastinoscopy	Stations 1–4, 7 (anterior mediastinal)
Extended cervical mediastinoscopy (ECM)	Stations 5, 6 (para-aortic)
Video-assisted mediastinoscopic lymphadenectomy (VAMLA)	Stations 7, 8
Chamberlain procedure (anterior mediastinotomy)	Station 5 (aortopulmonary window)
Endobronchial ultrasound (EBUS)-guided needle aspiration	Stations 2R/2L, 4R/4L, 7, and 10
Endoscopic ultrasound (EUS)-guided needle aspiration	Stations 4L, 7–9
Video-assisted thoracoscopic surgery (VATS)	Ipsilateral mediastinal nodes

noscopy. Limitations to access to relevant lymph node stations may impact the number of false-negative results with this technique and its sensitivity.

The sensitivity of standard mediastinoscopy is 81% (range 40–97%) while its specificity and PPV are both 100% and the NPV is 91% (Table 8.6). The number of accessible lymph node stations has been increased by enhancements of the standard mediastinoscopy technique, including extended cervical mediastinoscopy (ECM: can access stations 5 and 6), and video-assisted mediastinoscopic lymphadenectomy (VAMLA: can access stations 7 and 8). These enhancements have resulted in a sensitivity of 96% as well as a specificity of 100%, with almost unchanged morbidity and mortality [54].

8.3.2 Endoscopic Techniques

Endoscopic techniques are minimally invasive and provide histological or cytological confirmation of nodal involvement. By the combination of endoscopic ultrasound (EUS) and endobronchial ultrasound (EBUS) with PET/CT imaging, similar results can be achieved as for mediastinoscopy. The benefits of an endosonographic diagnosis are based on its low morbidity and mortality, which have been shown to be 2% and 0.08%, respectively, with mediastinoscopy [57]. Furthermore, these techniques are less costly than VMS.

Transbronchial needle aspiration (TBNA) has been shown to be a safe procedure and is useful in patients with enlarged mediastinal lymph nodes. However, this so-called blind or unguided technique has a moderate yield and is reliant on the experience of the investigator. Furthermore, the results of TBNA depend on the size of the lymph node (>15–20 mm short axis on CT scan). Although TBNA is mostly used to obtain subcarinal lymph node biopsies, it may also be used to obtain paratracheal lymph node biopsies. Paratracheal lymph nodes may sometimes be harder to access because of the difficulty of sufficiently angulating the bronchoscope and the needle. In an overview, TNBA had a sensitivity of 78% (range 14–100%) and a false-negative rate of 29% in cN2 disease [24]. Similar sensitivity and false-negative rates were reported in another overview by Lardinois [53] (Table 8.6). This high false-negative rate has limited the use of conventional TBNA for complete mediastinal lymph node staging. Conventional TBNA is useful if it leads to proof of N3 disease, but too often does not exclude N3 disease in cases of proven N2 disease.

The accuracy of TBNA can be improved by the use of endoscopic ultrasonography guidance techniques like EBUS-guided TBNA (EBUS-TBNA) or EUS-guided fine-needle aspiration (EUS-FNA) either alone or in combination. A recent meta-analysis of EUS-FNA alone, EBUS-TBNA alone, and EUS/EBUS combined has reported a pooled sensitivity and specificity of 86% and 100%, respectively, for mediastinal staging of lung cancer [56]. EBUS can be used to access lymph node stations 2R/2L, 4R/4L, 7, and 10 (hilar lymph nodes) as shown in Table 8.7. EUS particularly visualizes superior mediastinal lymph nodes in station 4L and inferior mediastinal nodes in stations 7, 8, and 9. Thus, EUS-FNA complements other techniques, as it can visualize lymph nodes (i.e., in stations 8 and 9) that are not

accessible by EBUS-TBNA or mediastinoscopy. Lymph node stations 5 and 6 can be well visualized by EUS but are rarely sampled without traversing the pulmonary artery/aorta. Lymph node stations 5 and 6 are predominantly affected by left upper lobe tumors and the surgical staging method of choice for such nodes is video-assisted thoracoscopic surgery (VATS).

8.3.3 Current Guidelines for Primary Mediastinal Staging

The current guidelines for primary mediastinal staging of NSCLC provided by the European Society of Thoracic Surgeons (ESTS) [20] are visualized in Fig. 8.15. Endosonography is recommended over surgical staging as the initial procedure for mediastinal nodal staging in patients with suspected or proven NSCLC with abnormal mediastinal and/or hilar nodes at CT, PET, or PET/CT. The combination of EBUS-TBNA and EUS-FNA is preferred over either test alone. Endoscopic needle techniques have sensitivities of approximately 90% when used in combination with ultrasound (EUS, EBUS). In direct comparison with surgical staging, they have emerged as the best first diagnostic tools to obtain tissue. However, in cases where the clinical suspicion of mediastinal lymph node involvement remains high after a negative result using a needle technique, surgical staging like mediastinoscopy or video-assisted thoracoscopic surgery (VATS) should be performed. In particular, patients with small mediastinal lymph nodes without FDG

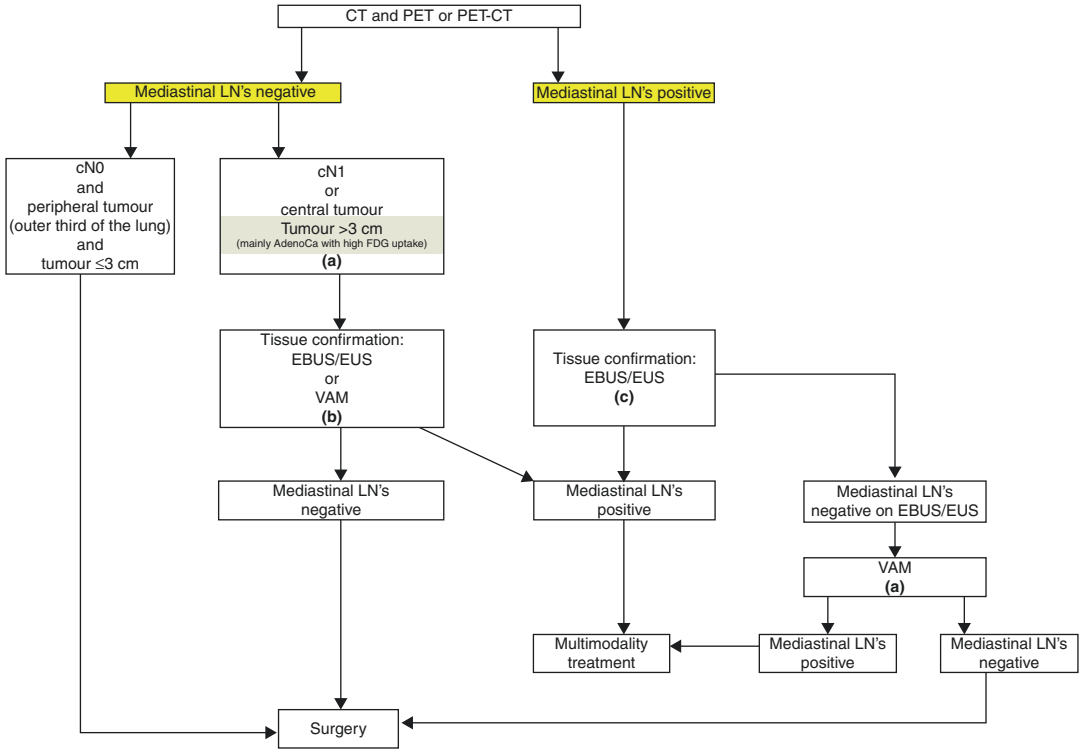

(a) : In tumours > 3 cm (mainly in adenocarcinoma with high FDG uptake) invasive staging should be considered
(b) : Depending on local expertise to adhere to minimal requirements for staging
(c) : Endoscopic techniques are minimally invasive and are the first choice if local expertise with EBUS/EUS needle aspiration is available
(d) : Due to its higher NPV, in case of PET positive or CT enlarged mediastinal LN's, videoassisted mediastinoscopy (VAM) with nodal dissection or biopsy remain indicated when endoscopic staging is negative. Nodal dissection has an increased accuracy over biopsy

Fig. 8.15 Revised ESTS guidelines for primary mediastinal staging. Reprinted from [20] with permission from Oxford University Press

uptake present a 6–30% risk of having mediastinal metastases in the following cases:

- Enlarged or FDG-avid hilar lymph nodes, or small and FDG-avid hilar lymph nodes
- Non-FDG-avid lung tumor (i.e., pulmonary carcinoid, pulmonary adenocarcinoma in situ)
- Lung tumor >3 cm (mainly in the case of adenocarcinoma with high FDG uptake) without any lymph node involvement at CT or PET

In these cases, mediastinal staging should be performed for accurate mediastinal nodal assessment in order to allocate patients appropriately for therapy with curative intent.

Mediastinal lymph node metastases are present in less than 6% of patients with small peripheral tumors that present with neither enlarged nor FDG-avid hilar or mediastinal lymph nodes [58]. It is therefore suggested in the guidelines that for patients with a peripheral clinical stage IA tumor (i.e., negative nodal involvement by FDG-PET/CT) no invasive preoperative evaluation of the mediastinal nodes is required.

For patients with a left upper lobe tumor in whom invasive mediastinal staging is indicated (as defined in previous recommendations), it is suggested that invasive assessment of the APW nodes be performed (via Chamberlain procedure, VATS, or extended cervical mediastinoscopy) if other mediastinal node stations are found to be uninvolved [24]. N1 nodes are usually resected with the primary tumor, if complete surgical resection is undertaken.

Since the effectiveness of endoscopic (EUS/EBUS) and mediastinoscopic techniques relies heavily on the experience of the examiner/operator, the choice between these techniques for use in mediastinal staging should be based on available expertise. Moreover, the surgical staging techniques (e.g., VMS, VATS, or Chamberlain procedure) should be considered as complementary more than competing methods. To ensure the most accurate staging in treatment centers, all noninvasive imaging techniques and invasive surgical and minimally invasive needle-based endoscopic staging techniques should be available.

Due to the low negative predictive value of EBUS or EUS in the event of negative results it is necessary to subsequently conduct a mediastinoscopic lymph node biopsy. In the case of a low probability of a targeted diagnosis by endoscopy initially, a mediastinoscopical approach should be conducted primarily, in order to avoid double examinations. This is especially important for clinical stages with central tumors, including stage cN2 or cN3 disease. In the case of a positive PET/CT result, a confirmatory mediastinoscopy should always be performed. However, if the initial PET/CT is negative, a rate of 20% of false-negative results should be considered. Due to the low probability of positive results with EBUS/EUS when staging central tumors, mediastinoscopy should be conducted right away in these cases.

8.4 Limitations and Perspectives

Despite the most recent adaptation to the TNM staging system for non-small cell lung cancer, there are still a considerable number of limitations inherent to the current system. An important source of error lies in the data itself. Even though former limitations of an oligocentric database from a single country have been overcome, the gathering of suitable data for each revision remains challenging. This is particularly because treatment recommendations, as indirectly implicated in the TNM classification, should be derived whenever possible from properly conducted clinical trials.

The prognostic discriminatory power of any staging system is intimately connected to the level of sophistication of its underlying database, which, in turn, is determined by the structure of the previous staging classification and the therapeutic concepts available at the time. The backward compatibility of a redefined staging system to its predecessors is generally limited, depending on the extent of changes that have been applied. As a consequence of the aforesaid, a newly revised staging classification will be of limited help for any decision on treatment strategies that have not contributed to its underlying

database, a situation that currently applies to the different sorts of novel targeted therapies, in particular.

Another important limitation of the TNM staging system is that the information used for staging is purely anatomic and as such does not capture any prognostic information that is unrelated to the anatomic extent of the disease. This applies to all sorts of parameters obtained from blood samples and other laboratory tests, such as tumor markers, as well as clinical factors, such as performance status and comorbidities. Many selection criteria for modern therapy approaches, such as tumor type or genetic patterns, are therefore not covered by the TNM system. This gap between the TNM system and therapy decisions is getting even larger with the continuously increasing number of novel treatment options.

The ever-growing richness of detail of modern staging classifications also represents a challenge for the available imaging technologies in radiology and nuclear medicine. Remaining challenges are in particular the limited accuracy in the evaluation of mediastinal and chest wall infiltration for T staging, the decreased NPV of FDG-PET-negative lymph nodes in specific high-risk subgroups, and the generally low PPV of FDG-PET/CT for N staging [59]. Apart from higher anatomic resolution and image quality, the technical development of diagnostic imaging strongly focusses on the inclusion of "functional" image information, as well as on "molecular" and hybrid—morphologic and functional—imaging technologies. The most prominent examples for this development are CT perfusion [60], dual-energy CT [61], and hybrid FDG-PET/MRI [62, 63], where promising initial results have been published in recent years. The technical equipment required to perform these examinations, however, is still quite novel to clinical radiology and not yet available in every hospital. In consequence, the existing data on the staging performance of CT perfusion, dual-energy CT, and hybrid FDG-PET/MRI is scattered, mostly stemming from only a few different sites and obtained in limited numbers of patients. A much broader investigation of these methods in prospective interdisciplinary multicenter trials is required to tackle the persisting challenges for imaging-derived staging of NSCLC.

References

1. World Health Organization. International Agency for Research on Cancer. GLOBOCAN 2012: Estimated Cancer Incidence, Mortality and Prevalence Worldwide in 2012. Lung Cancer. http://globocan.iarc.fr/Pages/fact_sheets_cancer.aspx. Accessed 7 May 2017.
2. U.S. National Institutes of Health. National Cancer Institute: SEER Cancer Statistics Review, 1975–2012. http://seer.cancer.gov/csr/1975_2012/browse_csr.php?sectionSEL=15&pageSEL=sect_15_table.28.html. Accessed 7 May 2017.
3. Denoix P. Enquête permanente dans les centres anticancéreux. Bull Inst Natl Hyg. 1946;1:70–5.
4. Goldstraw P, Chansky K, Crowley J, et al. International Association for the Study of Lung Cancer Staging and Prognostic Factors Committee, Advisory Boards, and Participating Institutions.; International Association for the Study of Lung Cancer Staging and Prognostic Factors Committee Advisory Boards and Participating Institutions. The IASLC Lung Cancer Staging Project: Proposals for Revision of the TNM Stage Groupings in the Forthcoming (Eighth) Edition of the TNM Classification for Lung Cancer. J Thorac Oncol. 2016;11(1):39–51.
5. Birley JD, Gospodarowicz M, Wittekind C, editors. TNM classification of malignant tumours. 8th ed. Oxford: Wiley-Blackwell; 2016.
6. Sobin L, Gospodarowicz M, Wittekind C, editors. TNM classification of malignant tumours. 7th ed. Oxford: Wiley-Blackwell; 2009.
7. Rusch VW, Asamura H, Watanabe H, et al. The IASLC lung cancer staging project: a proposal for a new international lymph node map in the forthcoming eventh edition of the TNM classification for ung cancer. J Thorac Oncol. 2009;4(5):568–77.
8. Mountain CF, Dresler CM. Regional lymph node classification for lung cancer staging. Chest. 1997;111(6):1718–23.
9. The Japan Lung Cancer Society. Classification of lung cancer. Tokyo: Kanehara & Co; 2000.
10. Rami-Porta R, Bolejack V, Crowley J, et al. IASLC Staging and Prognostic Factors Committee, Advisory Boards and Participating Institutions. The IASLC Lung Cancer Staging Project: Proposals for the Revisions of the T Descriptors in the Forthcoming Eighth Edition of the TNM Classification for Lung Cancer. J Thorac Oncol. 2015;10(7):990–1003.
11. Eberhardt WE, Mitchell A, Crowley J, Kondo H, Kim YT, Turrisi A 3rd, Goldstraw P, Rami-Porta R, International Association for Study of Lung Cancer Staging and Prognostic Factors Committee, Advisory Board Members, and Participating Institutions. The

IASLC Lung Cancer Staging Project: Proposals for the Revision of the M Descriptors in the Forthcoming Eighth Edition of the TNM Classification of Lung Cancer. J Thorac Oncol. 2015;10(11):1515–22.
12. Goldstraw P, Crowley J, IASCL International Lung Cancer Staging Project. The IASCL international project on lung cancer. J Thorac Oncol. 2006;1:208–86.
13. Nair A, Klusmann MJ, Kirupa H, Jogeesvaran H, Grubnic S, Green SJ, Vlahos I. Revisions to the TNM. Staging of non–small cell lung cancer: rationale, clinicoradiologic implications, and persistent limitations. Radiographics. 2011;31:215–38.
14. Rami-Porta R, Asamura H, Goldstraw P. Predicting the prognosis of lung cancer: the evolution of tumor, node and metastasis in the molecular age—challenges and opportunities. Transl Lung Cancer Res. 2015;4(4):415–23.
15. Rami-Porta R, Bolejack V, Giroux DJ, Chansky K, Crowley J, Asamura H, Goldstraw P, International Association for the Study of Lung Cancer Staging and Prognostic Factors Committee, Advisory Board Members and Participating Institutions. The IASLC lung cancer staging project: the new database to inform the eighth edition of the TNM classification of lung cancer. J Thorac Oncol. 2014;9(11):1618–24.
16. MacMahon H, Naidich DP, Goo JM, et al. Guidelines for management of incidental pulmonary nodules detected on CT images: from the Fleischner Society 2017. Radiology. 2017;23:161659. https://doi.org/10.1148/radiol.2017161659.
17. Travis WD, Asamura H, Bankier AA, et al. International Association for the Study of Lung Cancer Staging and Prognostic Factors Committee and Advisory Board Members. The IASLC Lung Cancer Staging Project: Proposals for Coding T Categories for Subsolid Nodules and Assessment of Tumor Size in Part-Solid Tumors in the Forthcoming Eighth Edition of the TNM Classification of Lung Cancer. J Thorac Oncol. 2016;11(8):1204–23.
18. The National Lung Screening Trial Research Team. Results of initial low-dose computed tomographic screening for lung cancer. N Engl J Med. 2013;368:1980–91.
19. Horeweg N, Scholten ET, de Jong PA, et al. Detection of lung cancer through low-dose CT screening (NELSON): a prespecified analysis of screening test performance and interval cancers. Lancet Oncol. 2014;15:1342–50.
20. De Leyn P, Dooms C, Kuzdzal J, et al. Revised ESTS guidelines for preoperative mediastinal lymph node staging for non-small-cell lung cancer. Eur J Cardiothorac Surg. 2014;45(5):787–98.
21. De Wever W, Stroobants S, Coolen J, Verschakelen JA. Integrated PET/CT in staging non-small cell lung cancer: tech-nical aspects and clinical integration. Eur Respir J. 2009;33:201–12.
22. Pauls S, Buck AK, Hohl K, et al. Improved non-invasive T- staging in non-small cell lung cancer by integrated 18F-FDG PET/CT. Nuklearmedizin. 2007;46:9–14.
23. El-Sherief AH, Lau CT, Wu CC, Drake RL, Abbott GF, Rice TW. International Association for the Study of Lung Cancer (IASLC) lymph node map: radiologic review with CT illustration. Radiographics. 2014;34:1680–91.
24. Silvestri GA, Gonzalez AV, Jantz MA, Margolis ML, Gould MK, Tanoue LT, Harris LJ, Detterbeck FC. Methods for staging non-small cell lung cancer: diagnosis and management of lung cancer, 3rd ed: American College of Chest Physicians evidence-based clinical practice guidelines. Chest. 2013;143(5 Suppl):e211S–50S.
25. Gould MK, Kuschner WG, Rydzak CE, et al. Test erformance of positron emission tomography and computed tomography for mediastinal staging in patients with nonsmall-cell lung cancer: a meta-analysis. Ann Intern Med. 2003;39:879–92.
26. Dwamena BA, Sonnad SS, Angobaldo JO, Wahl RL. Metastases from non-small cell lung cancer: mediastinal staging in the 1990s–meta-analytic comparison of PET and CT. Radiology. 1999;213:530–6.
27. Toloza EM, Harpole L, McCrory DC. Noninvasive staging of non-small-cell lung cancer: a review of the current evidence. Chest. 2003;123(1 Suppl):137S–46S.
28. National Institute for Health and Clinical Excellence (NICE). NICE updates guidance on the diagnosis and treatment of lung cancer. https://www.nice.org.uk/guidance/cg121/chapter/1-Guidance#diagnosis-and-staging. Accessed 22 June 2017.
29. Boellaard R, Delgado-Bolton R, Oyen WJ, et al. European Association of Nuclear Medicine (EANM). FDG PET/CT: EANM procedure guidelines for tumour imaging: version 2.0. Eur J Nucl Med Mol Imaging. 2015;42(2):328–54.
30. Lardinois D, Weder W, Hany TF, et al. Staging of non-small-cell lung cancer with integrated positron-emission tomography and computed tomography. N Engl J Med. 2003;348:2500–7.
31. Madsen PH, Holdgaard PC, Christensen JB, et al. Clinical utility of F-18 FDG PET-CT in the initial evaluation of lung cancer. Eur J Nucl Med Mol Imaging. 2016;43:2084.
32. Fletcher JW, Kymes SM, Gould M, et al. A comparison of the diagnostic accuracy of 18F-FDG PET and CT in the characterization of solitary pulmonary nodules. J Nucl Med. 2008;49:179–85.
33. Sommer G, Wiese M, Winter L, Lenz C, Klarhöfer M, Forrer F, Lardinois D, Bremerich J. Preoperative staging of non-small-cell lung cancer: comparison of whole-body diffusion-weighted magnetic resonance imaging and 18F-fluorodeoxyglucose-positron emission tomography/computed tomography. Eur Radiol. 2012;22(12):2859–67.
34. Stroobants SG, D'Hoore I, Dooms C, et al. Additional value of whole-body fluorodeoxyglucose positron emission tomography in the detection of distant

metastases of non-small-cell lung cancer. Clin Lung Cancer. 2003;4:242–7.
35. Hsia TC, Shen YY, Yen RF, Kao CH, Changlai SP. Comparing whole body 18 F-2-deoxyglucose positron emission tomography and technetium-99m methylene diophosphate bone scan to detect bone metastases in patients with non-small cell lung cancer. Neoplasma. 2002;49(4):267–71.
36. Song JH, Chaudhry FS, Mayo-Smith WW. The incidental adrenal mass on CT: prevalence of adrenal disease in 1,049 consecutive adrenal masses in patients with no known malignancy. AJR Am J Roentgenol. 2008;190(5):1163–8.
37. Eggesbø HB, Hansen G. Clinical impact of adrenal expansive lesions in bronchial carcinoma. Acta Radiol. 1996;37(3 Pt 1):343–7.
38. Kaltenbach TE-M, Engler P, Kratzer W, et al. Prevalence of benign focal liver lesions: ultrasound investigation of 45,319 hospital patients. Abdominal Radiology. 2016;41:25–32.
39. Hillers TK, Sauve MD, Guyatt GH. Analysis of published studies on the detection of extrathoracic metastases in patients presumed to have operable non-small cell lung cancer. Thorax. 1994;49(1):14–9.
40. Hustinx R, Paulus P, Jacquet N, Jerusalem G, Bury T, Rigo P. Clinical evaluation of whole-body 18 F-fluorodeoxyglucose positron emission tomography in the detection of liver metastases. Ann Oncol. 1998;9(4):397–401.
41. Sommer G, Tremper J, Koenigkam-Santos M, et al. Lung nodule detection in a high-risk population: comparison of magnetic resonance imaging and low-dose computed tomography. Eur J Radiol. 2014;83(3):600–5.
42. Webb WR, Gatsonis C, Zerhouni EA, et al. CT and MR imaging in staging non-small cell bronchogenic carcinoma: report of the radiologic diagnostic oncology group. Radiology. 1991;178:705–13.
43. Yi CA, Lee KS, Lee HY, et al. Coregistered whole body magnetic resonance imaging-positron emission tomography (MRI-PET) versus PET-computed tomography plus brain MRI in staging resectable lung cancer: comparisons of clinical effectiveness in a randomized trial. Cancer. 2013;119:1784–91.
44. Ohno Y, Koyama H, Yoshikawa T, et al. Three-way comparison of whole-body MR, Coregistered whole-body FDG PET/MR, and integrated whole-body FDG PET/CT imaging: TNM and stage assessment capability for non-small cell lung cancer patients. Radiology. 2015;275:849–61.
45. Morikawa M, Demura Y, Ishizaki T, et al. The effectiveness of 18F-FDG PET/CT combined with STIR MRI for diagnosing nodal involvement in the thorax. J Nucl Med. 2009;50:81–7.
46. Takahara T, Imai Y, Yamashita T, et al. Diffusion weighted whole body imaging with background body signal suppression (DWIBS): technical improvement using free breathing, STIR and high resolution 3D display. Radiat Med. 2004;22:275–82.
47. Shen G, Lan Y, Zhang K, Ren P, Jia Z. Comparison of 18F-FDG PET/CT and DWI for detection of mediastinal nodal metastasis in non-small cell lung cancer: a meta-analysis. PLoS One. 2017;12(3):e0173104.
48. Hochstenbag MM, Twijnstra A, Hofman P, Wouters EF, ten Velde GP. MR-imaging of the brain of neurologic asymptomatic patients with large cell or adenocarcinoma of the lung. Does it influence prognosis and treatment? Lung Cancer. 2003;42(2):189–93.
49. Earnest F IV, Ryu JH, Miller GM, et al. Suspected non small cell lung cancer: incidence of occult brain and skeletal metastases and effectiveness of imaging for detection—pilot study. Radiology. 1999;211(1):137–45.
50. Yokoi K, Kamiya N, Matsuguma H, et al. Detection of brain metastasis in potentially operable non-small cell lung cancer: a comparison of CT and MRI. Chest. 1999;115(3):714–9.
51. Van den Wyngaert T, Strobel K, Kampen WU, et al. The EANM practice guidelines for bone scintigraphy. Eur J Nucl Med Mol Imaging. 2016;43:1723–38.
52. Robinson LA, Wagner H Jr, Ruckdeschel JC, American College of Chest Physicians. Treatment of stage IIIA non-small cell lung cancer. Chest. 2003;123(1 Suppl):202S–20S.
53. Lardinois D. Pre- and intra-operative mediastinal staging in non-small-cell lung cancer. Swiss Med Wkly. 2011;141:w13168.
54. Zielinski M, Szlubowski A, Kołodziej M, Orzechowski S, Laczynska E, Pankowski J, Jakubiak M, Obrochta A. Comparison of endobronchial ultrasound and/or endoesophageal ultrasound with transcervical extended mediastinal lymphadenectomy for staging and restaging of non-small-cell lung cancer. J Thorac Oncol. 2013;8(5):630–6.
55. Um SW, Kim HK, Jung SH, et al. Endobronchial ultrasound versus mediastinoscopy for mediastinal nodal staging of non-small-cell lung cancer. J Thorac Oncol. 2015;10(2):331–7.
56. Zhang R, Ying K, Shi L, Zhang L, Zhou L. Combined endobronchial and endoscopic ultrasound-guided fine needle aspiration for mediastinal lymph node staging of lung cancer: a meta-analysis. Eur J Cancer. 2013;49(8):1860–7.
57. Van Schill PE, et al. Surgical treatment of early-stage non-small-cell lung cancer. EJC Suppl. 2013;11(2):110–22.
58. Tournoy KG, Keller SM, Annema JT. Mediastinal staging of lung cancer: novel concepts. Lancet Oncol. 2012;13:e221–9.
59. Sommer G, Stieltjes B. Magnetic resonance imaging for staging of non-small-cell lung cancer—technical advances and unmet needs. J Thorac Dis. 2015;7(7):1098–102.

60. Ippolito D, Capraro C, Guerra L, De Ponti E, Messa C, Sironi S. Feasibility of perfusion CT technique integrated into conventional ^{18}FDG/PET-CT studies in lung cancer patients: clinical staging and functional information in a single study. Eur J Nucl Med Mol Imaging. 2013;40(2):156–65.
61. Sudarski S, Hagelstein C, Weis M, Schoenberg SO, Apfaltrer P. Dual-energy snap-shot perfusion CT in suspect pulmonary nodules and masses and for lung cancer staging. Eur J Radiol. 2015;84(12):2393–400.
62. Schwenzer NF, Schraml C, Müller M, et al. Pulmonary lesion assessment: comparison of whole-body hybrid MR/PET and PET/CT imaging—pilot study. Radiology. 2012;264:551–8.
63. Heusch P, Buchbender C, Köhler J, et al. Thoracic staging in lung cancer: prospective comparison of 18F-FDG PET/MR imaging and 18F-FDG PET/CT. J Nucl Med. 2014;55:373–8.